Jurkat cells and human primary $CD4^+$ T cells, which demonstrated pronounced decreases in virus particle production in SOCS1-siRNA-expressed cells compared with the controls (Fig. 4 *G* and *H*). These results together indicate that the specific inhibition of SOCS1 suppresses the optimal trafficking of Gag to PM, resulting in the degradation of Gag in lysosomes, which in turn leads to the efficient and reproducible inhibition of HIV-1 particle production in various types of human cells.

Discussion

In this work, we report that SOCS1 is an inducible host factor during HIV-1 infection and plays a key role in the late stages of the viral replication pathway via an IFN-independent mechanism (SI Fig. 6). These results represent evidence that SOCS1 is a potent host factor that facilitates HIV-1 particle production via posttranscriptional mechanisms.

SOCS1 has been shown to be a suppressor of several cytokine signaling pathways, and like all SOCS family members it has a central SH2 domain and a conserved C-terminal domain known as the SOCS box (21, 22). Structure–function analyses have further demonstrated that the SOCS1 SH2 domain is required for the efficient binding of its substrates (23, 24). Indeed, our current analyses have also revealed that the SH2 domain of SOCS1 is required for its interaction with the HIV-1 Gag protein. We have shown from our present data that the SOCS box is also required for SOCS1 to function during HIV-1 particle production.

The SOCS box-mediated function of SOCS1 is chiefly exerted via its ubiquitin ligase activity (21, 25). Biochemical binding studies have shown that the SOCS box of SOCS1 interacts with the elongin BC complex, a component of the ubiquitin/proteasome pathway that forms an E3 ligase with Cul2 (or Cul5) and Rbx-1 (21, 26, 27). We show from our current experiments that the SOCS box is required for HIV-1 particle production, indicating the involvement of the ubiquitin/proteasome pathway. However, it is still unknown whether SOCS1 promotes the ubiquitination of Gag and, if so, whether the mono- or poly-ubiquitination of Gag would affect its trafficking and protein stability. Further studies will be necessary to clarify the biological significance of Gag ubiquitination.

Perlman and Resh (20) recently reported that newly synthesized Gag first appears to be diffusely distributed in the cytoplasm, accumulates in perinuclear clusters, passes transiently through a MVB-like compartment, and then traffics to PM. Consistent with these observations, our current work also shows that Gag is accumulated at perinuclear clusters as solid aggregates when its targeting to PM is impaired because of the SOCS1 inhibition.

Another aspect of SOCS1 function during HIV-1 infection was proposed recently. Song *et al.* (28) reported that SOCS1-silenced dendritic cells broadly induce the enhancement of HIV-1 Env-specific $CD8^+$ cytotoxic T lymphocytes and $CD4^+$ T helper cells as well as an antibody response. The induction of the SOCS1 gene in HIV-1 infected cells might therefore disrupt a specific intracellular immune response to HIV-1 in infected host cells.

Based on the strong evidence that we present in our current work that SOCS1 positively regulates the late stages of HIV replication, we conclude that SOCS1 is likely to be a valuable therapeutic target not only for future treatments of AIDS and related diseases, but also for a postexposure prophylaxis against disease in HIV-1-infected individuals.

Materials and Methods

Antibodies and Fluorescent Reagents. Antibodies and fluorescent reagents were obtained from the following sources. Anti-CD63, anti-AP-3, anti-myc (A-14), and anti-SOCS1 (H-93) were from Santa Cruz Biotechnology. Anti-SOCS1 was from Zymed Laboratories. Anti-FLAG (M2) and anti-HA (12CA5) were from Sigma and Roche Diagnostics, respectively. Anti-HIV-p24 (Dako; Cytomation), anti-STAT1, and anti-phospho-STAT1 (Y701) were from BD Transduction Laboratories. Sheep polyclonal anti-TGN46 was from GeneTex.

Plasmid Constructs. Expression constructs for SOCS1 have been described in ref. 29. GST fusion constructs with specific regions derived from the codon-optimized *gag* were generated (MA, CA, NC, p6, Δp6, full-length Gag) by cloning into pGEX-2T (GE Healthcare Bio-Sciences) as described in ref. 30. For retrovirus-mediated siRNA expression, pSUPER.retro.puro vector was digested, as described in ref. 31, with the following sequences: SOCS1-siRNAI, TCGAGCTGCTGGAGCACTA; SOCS1-siRNAII, GGCCAGAACCTTCCTCCTCTT; control siRNA, TCGTATGTTGTGTGGAATT.

Electron Microscopy. Transfected 293T cells were fixed with 2.5% glutaraldehyde and subjected to TEM, as described (14, 32).

ACKNOWLEDGMENTS. We thank Dr. H Gottlinger (University of Massachusetts) for providing plasmids. This work was supported in part by grants from the Ministry of Education, Culture, Sports, Science, and Technology of Japan and Human Health Science of Japan.

1. Sorin M, Kalpana GV (2006) *Curr HIV Res* 4:117–130.
2. Freed EO (2004) *Trends Microbiol* 12:170–177.
3. Peterlin BM, Trono D (2003) *Nat Rev Immunol* 3:97–107.
4. Trkola A (2004) *Curr Opin Microbiol* 7:555–559.
5. Freed EO (1998) *Virology* 251:1–15.
6. Adamson CS, Jones IM (2004) *Rev Med Virol* 14:107–121.
7. VerPlank L, Bouamr F, LaGrassa TJ, Agresta B, Kikonyogo A, Leis J, Carter CA (2001) *Proc Natl Acad Sci USA* 98:7724–7729.
8. Garrus JE, von Schwedler UK, Pornillos OW, Morham SG, Zavitz KH, Wang HE, Wettstein DA, Stray KM, Cote M, Rich RL, *et al.* (2001) *Cell* 107:55–65.
9. Strack B, Calistri A, Craig S, Popova E, Gottlinger HG (2003) *Cell* 114:689–699.
10. Dong X, Li H, Derdowski A, Ding L, Burnett A, Chen X, Peters TR, Dermody TS, Woodruff E, Wang JJ, *et al.* (2005) *Cell* 120:663–674.
11. Alroy I, Tuvia S, Greener T, Gordon D, Barr HM, Taglicht D, Mandil-Levin R, Ben-Avraham D, Konforty D, Nir A, *et al.* (2005) *Proc Natl Acad Sci USA* 102:1478–1483.
12. Ryo A, Suzuki Y, Ichiyama K, Wakatsuki T, Kondoh N, Hada A, Yamamoto M, Yamamoto N (1999) *FEBS Lett* 462:182–186.
13. Adachi A, Gendelman HE, Koenig S, Folks T, Willey R, Rabson A, Martin MA (1986) *J Virol* 59:284–291.
14. Demirov DG, Ono A, Orenstein JM, Freed EO (2002) *Proc Natl Acad Sci USA* 99:955–960.
15. Chang TL, Mosoian A, Pine R, Klotman ME, Moore JP (2002) *J Virol* 76:569–581.
16. De Sepulveda P, Okkenhaug K, Rose JL, Hawley RG, Dubreuil P, Rottapel R (1999) *EMBO J* 18:904–915.
17. Kamio M, Yoshida T, Ogata H, Douchi T, Nagata Y, Inoue M, Hasegawa M, Yonemitsu Y, Yoshimura A (2004) *Oncogene* 23:3107–3115.
18. Gallina A, Mantoan G, Rindi G, Milanesi G (1994) *Biochem Biophys Res Commun* 204:1031–1038.
19. Accola MA, Strack B, Gottlinger HG (2000) *J Virol* 74:5395–5402.
20. Perlman M, Resh MD (2006) *Traffic* 7:731–745.
21. Alexander WS (2002) *Nat Rev Immunol* 2:410–416.
22. Marine JC, Topham DJ, McKay C, Wang D, Parganas E, Stravopodis D, Yoshimura A, Ihle JN (1999) *Cell* 98:609–616.
23. Narazaki M, Fujimoto M, Matsumoto T, Morita Y, Saito H, Kajita T, Yoshizaki K, Naka T, Kishimoto T (1998) *Proc Natl Acad Sci USA* 95:13130–13134.
24. Yasukawa H, Misawa H, Sakamoto H, Masuhara M, Sasaki A, Wakioka T, Ohtsuka S, Imaizumi T, Matsuda T, Ihle JN, *et al.* (1999) *EMBO J* 18:1309–1320.
25. Tyers M, Rottapel R (1999) *Proc Natl Acad Sci USA* 96:12230–12232.
26. Kamizono S, Hanada T, Yasukawa H, Minoguchi S, Kato R, Minoguchi M, Hattori K, Hatakeyama S, Yada M, Morita S, *et al.* (2001) *J Biol Chem* 276:12530–12538.
27. Kamura T, Burian D, Yan Q, Schmidt SL, Lane WS, Querido E, Branton PE, Shilatifard A, Conaway RC, Conaway JW (2001) *J Biol Chem* 276:29748–29753.
28. Song XT, Evel-Kabler K, Rollins L, Aldrich M, Gao F, Huang XF, Chen SY (2006) *PLoS Med* 3:e11.
29. Ryo A, Suizu F, Yoshida Y, Perrem K, Liou YC, Wulf G, Rottapel R, Yamaoka S, Lu KP (2003) *Mol Cell* 12:1413–1426.
30. Morikawa Y, Kishi T, Zhang WH, Nermut MV, Hockley DJ, Jones IM (1995) *J Virol* 69:4519–4523.
31. Ryo A, Uemura H, Ishiguro H, Saitoh T, Yamaguchi A, Perrem K, Kubota Y, Lu KP, Aoki I (2005) *Clin Cancer Res* 11:7523–7531.
32. Nagashima Y, Nishihira H, Miyagi Y, Tanaka Y, Sasaki Y, Nishi T, Imaizumi K, Aoki I, Misugi K (1996) *Cancer* 77:799–804.

Published online 29 October 2008

Nucleic Acids Research, 2008, Vol. 36, No. 21 ***6859–6871***
doi:10.1093/nar/gkn802

The antiretroviral potency of APOBEC1 deaminase from small animal species

Terumasa Ikeda[1,2], Takeo Ohsugi[3], Tetsuya Kimura[1], Shuzo Matsushita[4], Yosuke Maeda[2], Shinji Harada[2] and Atsushi Koito[1,*]

[1]Department of Retrovirology and Self-Defense, Faculty of Medical and Pharmaceutical Sciences, [2]Department of Medical Virology, Faculty of Medical and Pharmaceutical Sciences, [3]Center for Animal Resources and Development, Institute of Resource Development and Analysis and [4]Center for AIDS Research, Kumamoto University, Kumamoto 860-8556, Japan

Received August 28, 2008; Revised October 7, 2008; Accepted October 11, 2008

ABSTRACT

Although the role of the APOBEC3-dependent retroelement restriction system as an intrinsic immune defense against human immunodeficiency virus type1 (HIV-1) infection is becoming clear, only the rat ortholog of mammalian APOBEC1s (A1) thus far has been shown to possess antiviral activity. Here, we cloned A1 cDNAs from small animal species, and showed that similar to rat A1, both wild-type and Δ*vif* HIV-1 infection was inhibited by mouse and hamster A1 (4- to 10-fold), whereas human A1 had negligible effects. Moreover, rabbit A1 significantly reduced the infectivity of both HIV-1 virions (>300-fold), as well as that of SIVmac, SIVagm, FIV and murine leukemia virus. Immunoblot analysis showed that A1s were efficiently incorporated into the HIV-1 virion, and their packaging is mediated through an interaction with the nucleocapsid Gag domain. Interestingly, there was a clear accumulation of particular C-T changes in the genomic RNAs of HIV-1 produced in their presence, with few G-A changes in the proviral DNA. Together, these data reveal that A1 may function as a defense mechanism, regulating retroelements in a wide range of mammalian species.

INTRODUCTION

It is now clear that the scope of intracellular defense mechanisms against retroviral infections extend beyond the conventional innate and acquired immune responses, involving a series of dominant inhibitory activities that influence retroviral tropism. Two major restriction factors identified thus far are the early block owing to Fv1 and TRIM5α that target incoming retroviral capsids, and cytidine deaminases, such as APOBEC3 (A3) that function at the late phase to hypermutate retroviral genome (1). The A3 proteins have been shown to inhibit the infectivity potential and mobility of a broad and growing number of exogenous retroviruses as well as endogenous retroelements (2,3). A3 edits deoxycytidine (dC) to deoxyuridine (dU) on nascent DNA minus strands during reverse transcription, but the mechanisms underlying the inhibitory effect on retroviruses are not fully understood.

The A3 encoded by mouse genome was found to be about ~30% identical to the human APOBEC3G (hA3G), initially identified as a critical target for the human immunodeficiency virus type1 (HIV-1) auxiliary protein Vif (4,5). Subsequently, anti-HIV activity of A3 was found to be maintained across diverse mammalian species, such as murine, cat and artiodactyls (cattle, pigs and sheep) in spite of extensive amino acid sequence divergence, and regardless of whether lentiviruses infect the species (5–8). However, the interaction of Vif with A3 molecules is species specific, and this Vif-resistant inhibition of HIV-1 by orthologous A3 proteins appears to contribute to restrict cells from nonprimate mammalian species to support productive HIV-1 replication. Thus, the removal of the A3-mediated block will be required for the development of a small animal model in which HIV-1 replicates efficiently.

Although the role of the A3-dependent retroelement restriction system as an intrinsic resistance mechanism is becoming clear, less well understood is mammalian APOBEC1 (A1), the catalytic component of a complex that deaminates apolipoprotein B mRNA in gastrointestinal tissues (9,10). It has been also shown that A1 exhibit potent DNA mutator activity in an *Escherichia coli* assay (11). Rodent A1s share ~70% amino acid sequence identity with human A1, but only rat homolog of A1 was shown to restrict HIV-1 independent of Vif (12,13). To address whether A1 orthologs are involved in an innate

*To whom correspondence should be addressed. Tel: +81 96 373 5133; Fax: +81 96 373 5132; Email: akoito@kumamoto-u.ac.jp

pathway of restriction of retrovirus infection, A1 cDNAs from small animal species were cloned, and expressed in order to examine their abilities to influence the infectivities of retroviral virions. Our studies show that several A1s from small animal species were efficiently incorporated into the HIV-1 virion via interaction with the nucleocapsid (NC) Gag domain, and suppressed HIV-1 replication in a cytidine deaminase dependent as well as independent manner. Interestingly, there was a clear accumulation of particular C-T changes in the genomic RNAs produced in the presence of rabbit A1, with few G-A changes in the proviral DNA. Moreover, the local mutational preferences on HIV-1 genomic RNA were found to be similar to those observed in apoB mRNA. Importantly, mutation of the catalytic residue Glu63 significantly reduced antiviral activity, and diminished G-A or C-T changes. Further, these deaminases also inhibited simian immunodeficiency virus (SIV)mac, SIVagm and feline immunodeficiency virus (FIV) infections and to a lesser extent murine leukemia virus (MLV). Together, these data reveal that, unlike their human counterparts, A1 in a wide range of mammalian species may function as a defense mechanism regulating retroelements.

MATERIALS AND METHODS

Molecular cloning of A1s

Primary tissues were prepared from small intestines, which had been removed aseptically from euthanatized ferret (*Mustela putorius furo*), rabbit (Kbt: NZW), hamster (Slc: Syrian) and mouse (C57BL/6N), respectively. Total RNA was prepared using TRIzol reagent (Invitrogen, Carlsbad, CA) and the synthesis of first strand cDNA was carried out with High Capacity cDNA Archive Kit (Applied Biosystems, Foster City, CA) using a random primer. cDNA from human small intestine and rat (Sprague-Dawley) liver was purchased from BD Biosciences Clontech, Palo Alto, CA (BD™ Marathon-Ready cDNA, Cat. #639326 and #639413, respectively). The cDNA encoding the entire open reading frame of the A1 were amplified using primer sets designated as seen in Table S1, based on A1 sequences from GeneBank except for ferret. Taq polymerase-amplified PCR products were cloned into pCR-Blunt (Invitrogen) vector and sequenced. The primary PCR product was subsequently reamplified by using oligonucleotides containing *Eco*RV and *Not*I cloning sites. Antisense primers encoded the hemagglutinin (HA)-epitope sequence YPYDVPDYA. Amplicons were cleaved at the restriction sites and ligated to similarly cleaved pCAGGS vector (14), yielding HA tagged A1 expression vectors. pCAGGS-based expression plasmids for HA-tagged hA3G has been described elsewhere (15). PCR products generated and digested as described above were also inserted into pcDNA 3.1/Zeo (Invitrogen).

Generation of catalytic site-mutated rabbit A1 expression vectors

Rabbit A1 catalytically inactive mutants E63A and E63Q were constructed with QuickChange® XL Site-Directed Mutagenesis Kit (Stratagene, La Jolla, CA) using oligonucleotide primers (Table S1), and inserted into pCAGGS vector.

Amino acid alignments and phylogenetic analysis

Protein sequences of full-length mammalian A1s were aligned with Clustal W software. Phylogenetic trees were reconstructed using the neighbor-joining method with 2000 bootstrap replications. MEGA 3.1 was used for phylogenetic analysis. The GenBank accession numbers of the A1 sequences used in these comparisons were rat (NM012907), mouse (NM031159), human (NM001644), opossum (NM001032982), rabbit (U10695), orangutan (AH013823), chimpanzee (XM001164661), rhesus monkey (XM001112583), cattle (XM594173), dog (XM543826), hamster (AF176577) and horse (XM001493159). The sequence of A1s reported in this article has been deposited in the GenBank data base (accession number AB425821).

Viral preparation and infectivity assay

293T, GP293, HeLa, Caco-2 and *Mus dunni* tail fibroblasts (MDTF) cells were maintained in DMEM supplemented with 10% fetal calf serum (Gibco, Grand Island, NY). VSV-G pseudotyped HIV-1-based luciferase reporter virus stocks were produced in 293T cells by cotransfection of wild-type or *Δvif* pNL4-3 Luc E^-R^- (5), together with pVSV-G and one of several expression vectors encoding APOBEC proteins, which are HA-epitope tagged or a control empty vector using Effectene® (Qiagen, Hilden, Germany). Culture supernatants were harvested, filtered and frozen in aliquots. The p24 content of the viruses was determined in ELISA kits (ZeptoMetrix, Buffalo, NY). Target fresh 293T cells were infected with 0.5–1.5 ng equivalent of luciferase reporter viruses and cultured for 48 h. Infected cells were lyzed, and each lysate was assayed for luciferase activity as previously described (16). Single-round SIVmac and SIVagm luciferase reporter virus stocks with or without Vif were produced as VSV-G pseudotypes in 293T cells by cotransfection of pSIV Luc E^-R^- or pSIV Luc E^-R^- *Δvif* (5) and an expression vectors for APOBECs or a mock vector. The p27 content of the viruses was determined in ELISA kits (ZeptoMetrix). Target fresh 293T cells were infected for with 4.0–80 ng equivalent of luciferase reporter viruses and cultured for 48 h. Infected cells were lyzed and each lysate was assayed for luciferase activity.

To generate FIV-GFP virus, 293T cells were transfected with pFIV-H1/copGFP and pFIV-34N (System Bioscience, Mountain View, CA), pVSV-G and APOBEC expression vector or an empty vector. Culture supernatants were filtered and centrifuged at 40 000*g* for 1 h. Target cells were infected with FIV-GFP viruses, equivalent to 8 ng of reverse transcriptase estimated by using Reverse Transcriptase Assay (Roche, Basel, Switzerland) and the infectivity was measured by flow cytometry at 48 h postinfection. Single-round MLV reporter virus stocks were produced as VSV-G pseudotypes in GP293 cells expressing Moloney MLV *gag* and *pol* genes (17) by cotransfection of pFB-Luc or pFB-hrGFP (Stratagene) together with expression vectors for APOBECs or a mock vector. Virus-containing supernatants were normalized for equal MLV p30 CA content estimated by Western analysis. Target MDTF cells were infected with equivalent amounts of MLV reporter viruses and cultured for 48 h. Values are presented as the percent

infectivity relative to the value of the wild-type virus without the expression of APOBECs.

Editing of HIV-1 proviral DNA and genomic RNA

The cells were harvested 48 h postinfection, and total DNA was isolated using the QIAamp DNA Blood Mini Kit (Qiagen). A 408 bp of the HIV-1 *pol* region was amplified with the high-fidelity DNA polymerase (Takara, Ohtsu, Japan) subsequent to the digestion with *DpnI*. Amplified fragments were subsequently gel purified, then cloned into pCR-Blunt vector (Invitrogen) and sequenced. The viral genomic RNA in cell-free virions was purified using QIAamp viral RNA Mini Kit (Qiagen) and converted to cDNA *in vitro* using a High Capacity cDNA Archive kit with random primers, sebsequent to the treatment with DNase. The *pol* region was amplified by PCR, cloned and sequenced as described above.

Western blot analysis

The encapsidation of APOBEC proteins into HIV-1 or MLV virions were detected by pelleting the supernatant of 293T cells transfected with viral DNA and HA-epitope tagged forms of the APOBEC expression vector through a 20% sucrose cushion. The pellets were solubilized in 50 µl of 1% Triton-containing buffer and the equivalent p24 of each solubilized virions was subjected to immunoblot analysis. Cell lysates, virion lysates and immunoprecipitates were subjected to SDS–PAGE, and then transferred to a PVDF membrane (Millipore, Bedford, MA). The membranes were probed with the anti-HA epitope (HA.11; Covance, Princeton, NJ) or anti-β-actin (AC-74; Sigma, Saint Louis, MO) antibody. A monoclonal antibody recognizing the p24 CA (18) and a goat anti-MLV p30 serum (ViroMed Biosafety Labs, Camden, NJ) was used for detection of HIV-1 and MLV CA, respectively. Reactive proteins were detected using biotin-conjugated rabbit immunoglobulin (Sigma), streptoavidin-conjugated peroxidase (Sigma) and developed using Chemi-Lumi One (Nacalai Tesque, Kyoto, Japan). The plasmids expressing HIV-1 Gag or the deletion mutants were described previously (22). Bands in western blots were quantified on a VersaDoc 5000 imager (BIO-RAD, Hercules, CA).

Nucleotide sequence accession numbers

The sequences determined in this study have been submitted to GenBank and assigned accession no. AB425821.

RESULTS

Molecular cloning and phylogenetic analysis of mammalian A1s

We cloned, sequenced and compared the predicted amino acid sequences of A1 cDNAs from primate (human), carnivora (ferret), lagomorphs (rabbit) and rodents (hamster, rat, mouse). Sequence analysis revealed that the clones obtained encoded genes that were identical to the GenBank sequences of A1s (rabbit;U10695, hamster; AF176577, rat;NM012907 and mouse;NM031159), except for one amino acid residue (M80I) substitution in human A1 (NM001644). Results showed that human A1 cDNA encodes an open reading frame of 236 amino acids that has a 78.0% amino acid sequence identity with ferret, 75.8% with rabbit and 70–72% with rodent orthologs. A short C-terminal extension was found in human and rabbit as previously reported (19), and also in ferrets but not in rodents. In particular, the active site motif, designated as His-X-Glu-$(X)_{23\text{-}28}$-Pro-Cys-X_2-Cys (X can be any amino acid) (20), was well conserved (Figure 1A). Phlyogenetic tree analyses revealed that the rabbit A1 gene is related to primate A1 genes, while A1s from rodents form a single separate cluster (Figure 1B).

A1s from small animal species inhibit HIV-1 virion infectivity

To examine the anti-HIV activities of A1s from these small animal species, single-round infectivity assay with VSV-G pseudotyped wild-type and *Δvif* HIV-1 luciferase reporter viruses (5) produced in the presence of the influenza HA epitope-tagged A1 proteins was performed. hA3G was used as a control in these experiments. To examine the effect on HIV-1 infectivity quantitatively, virions were normalized based on p24 content. Virus-induced intracellular luciferase activity, which is directly proportional to the infectivity of the virus, was measured 48 h after infection and calculated relative to the APOBEC-negative control virus (Figure 2A, Mock). As expected, hA3G caused a modest decrease in infectivity of the wild-type and a more pronounced decrease in infectivity of the *Δvif* HIV-1virus (Figure 2A). A1 from human intestine did not showed any antiviral activity, while, in agreement with previous observations (12,13), A1 from rat caused a relatively small (2- to 3-fold) decrease in infectivity of the *Δvif* HIV-1virus and a >5-fold decrease in infectivity of the wild-type virus (Figure 2A). In contrast with previous findings however (5,12,13), the A1s from rodents, such as hamster and mouse were equally active against wild-type and *Δvif* HIV-1 viruses, reducing their infectivity >10-fold in some experiments. A modest reduction in infectivity of wild-type and *Δvif* viruses was also found with A1 from ferrets, but of more interest are the findings with A1 from rabbits. Over 100-fold decrease in the *Δvif* HIV-1 virus and a more pronounced 300-fold decrease in infectivity of the wild-type virus was seen with this cytidine deaminase from rabbits. Identical results were obtained when rabbit A1 was expressed with an alternate expression vector, pcDNA3.1 (Figure S1), ruling out an effect specific to the pCAGGS construct used in these experiments. Dose titration studies showed that as little as 0.05 µg of rabbit A1 was sufficient to achieve significant inhibition against HIV-1 (Figure 2B), 10- to 20-fold more potent than APOBECs from other small animal species. For further confirmation, the anti-HIV activity of A1s from small animal species was examined with the use of a HIV-1-based the green fluorescent protein (GFP)-expressing reporter virus. As shown in Figure S2, the results obtained with the HIV-GFP vector are consistent with those seen using the HIV-Luc vector. These multiple lines of investigations indicate that, similar to hA3G, A1s from small animal species can function on HIV-1.

The cytidine deaminase domains of APOBEC proteins contains an active site with conserved consensus motifs in

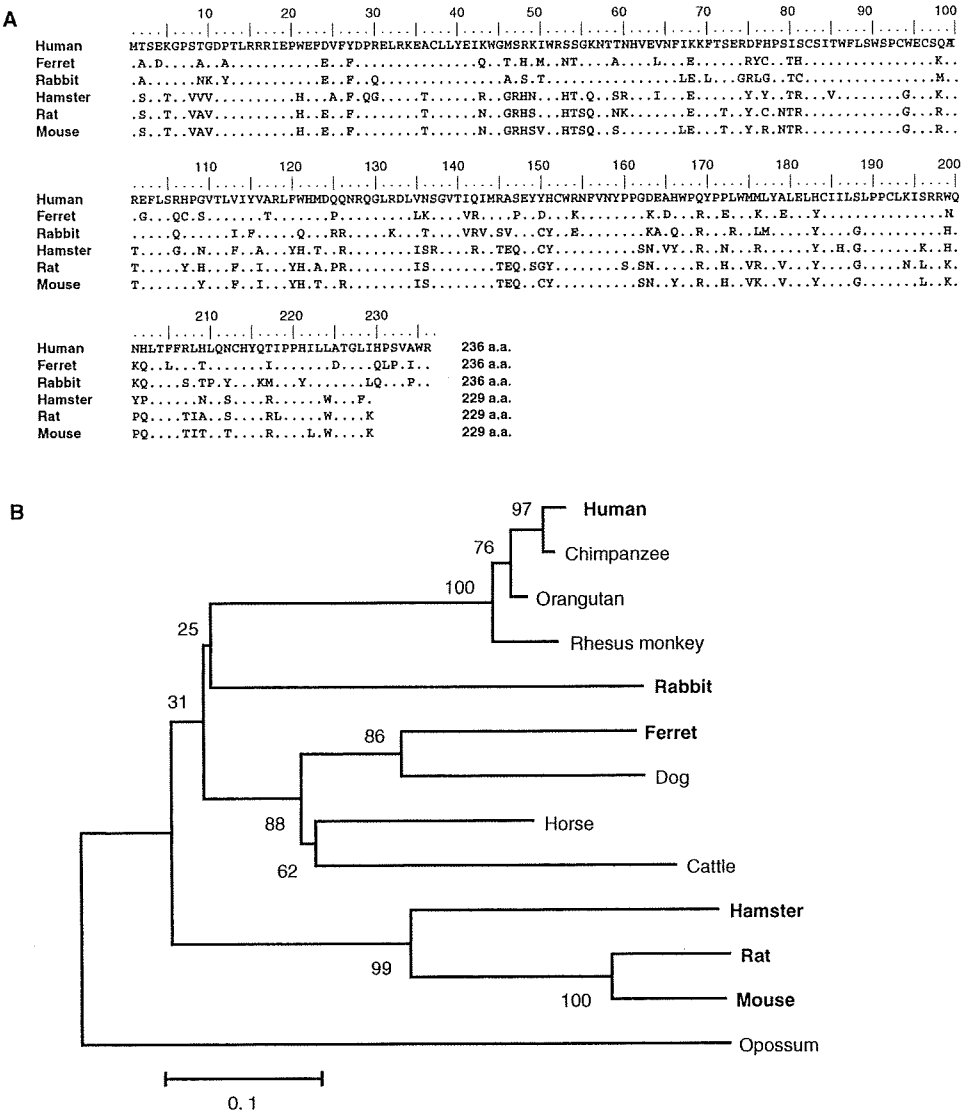

Figure 1. Alignment of the amino acid sequence and phylogenetic analysis of mammalian A1 proteins. (**A**) Amino acid sequence alignment of A1 from human, ferret, rabbit, hamstar, rat and mouse. The predicted amino acid sequences of these cloned A1 molecules are aligned with Clustal W software to the previously identified sequences of mammalian A1s. The numbers are amino acid residue positions. (**B**) Phylogenetic analysis of the protein sequences of full-length mammalian A1s. The tree was reconstructed by neighbor-joining method with protein *p*-distances using MEGA 3.1. Shown interior nodes are bootstrap percentages derived from 2000 replications. Branch lengths represent the number of substitution per site. Opossum is a separate group. The species used for further experiments in this study are indicated in bold letters.

which the His–Cys–Cys residues coordinate a Zn^{2+} ion, and the Glu residue serving an essential role in catalysis as a proton shuttle (21). Therefore, we generated the catalytic site mutant forms of rabbit A1 in which the critical Glu-63 of active site was changed to Ala or Gln (E63A, E63Q), and examined their antiviral activity. Results showed that the ability of the mutant proteins to restrict the infectivity of wild-type and *Δvif* viruses were severely, but not completely impaired (Figure 2C), suggesting the existence of an albeit weak deaminase-independent restriction mechanism by A1.

A1s are packaged into HIV-1 virions

It is now well established that human and murine A3s inhibit HIV-1 infectivity by being packaged into progeny virions. Therefore, we verified whether A1 proteins (which are epitope tagged) would indeed be selectively packaged into HIV-1 virions. For these studies, transfected cells were harvested, and proteins in whole-cell lysates were analyzed by western blotting with anti-HA, anti-HIV-1 CA p24 and anti-β-actin monoclonal antibodies with the β-actin blot serving as a loading control. Data showed comparable amounts of A1 proteins and HIV-1 Gag precursor protein (p55) expression, but minor effects on the processing efficiency into p24 CA with some A1 proteins (e.g. human and rabbit, Figure 2D). Cell-free virus was concentrated by pelleting through a 20% sucrose cushion, and then equivalent amount of solubilized virions was subjected into the western blotting. A1 proteins from small animal species were

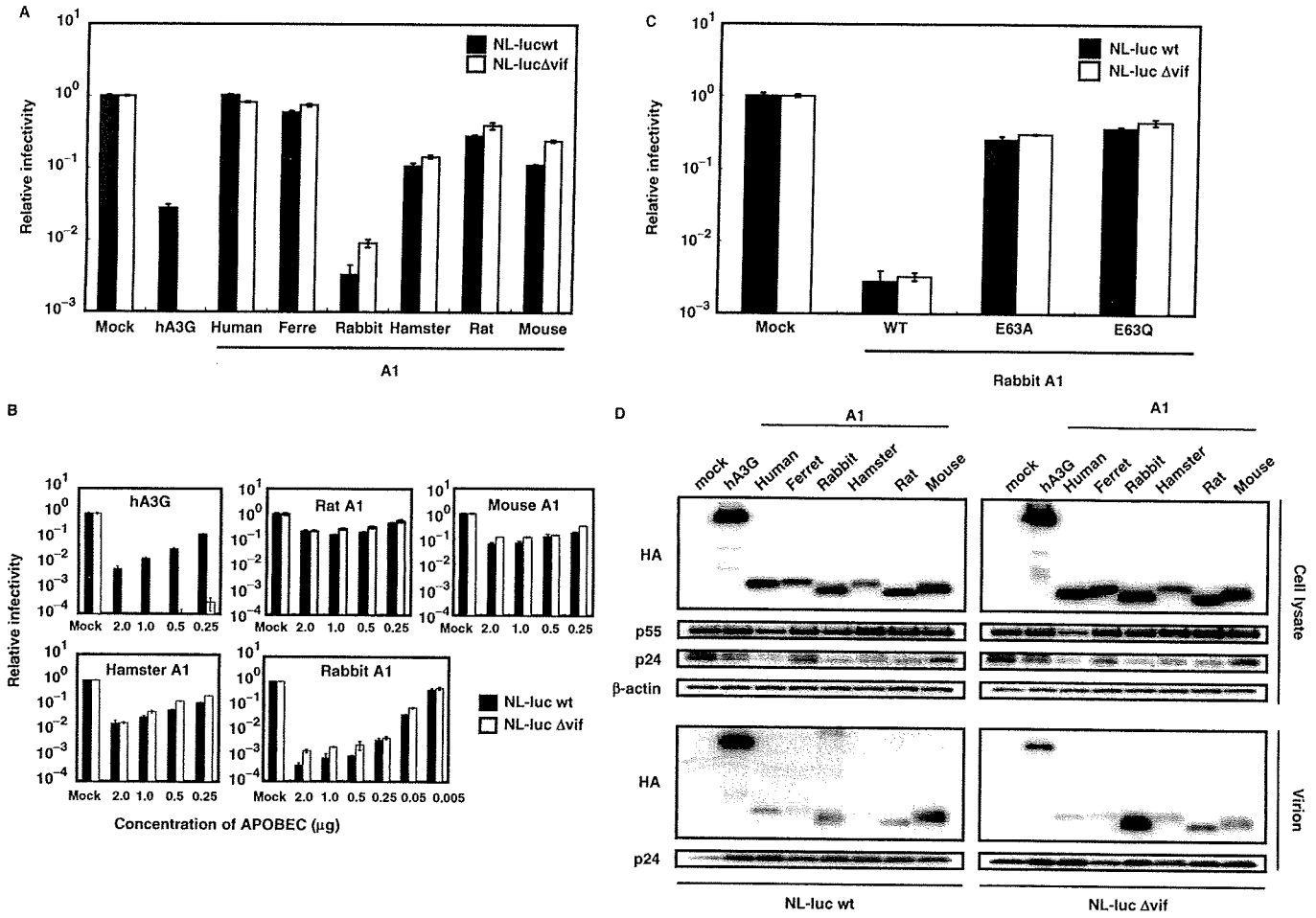

Figure 2. Inhibition of HIV-1 infection by A1s. (**A**) VSV-G pseudotyped wild-type and *Δvif* HIV-1 luciferase viruses were produced in 293T cells transfected with 1.5 μg of luciferase reporter viruses, 1.0 μg of pVSV-G and 0.5 μg of HA-tagged APOBEC expression vector or empty vector. Virus-containing supernatants were normalized for equal p24 content and used for the infection of the fresh 293T cells. Virus-induced intracellular luciferase activity was measured. Data are presented as a percentage of the level of luciferase activity detected in cells infected with virions derived from cells that did not express an exogenous APOBEC protein. The average of three experiments with standard deviation is indicated. (**B**) Wild-type and *Δvif* HIV-1 luciferase reporter viruses pseudotyped were produced in 293T cells transfected with decreasing amounts of HA-tagged APOBEC expression vector. The amount of expression vector plasmid transfected is shown in micro gram on the *X*-axis. (**C**) The catalysis domain of A1 is required for the efficient anti-HIV-1 potency of the rabbit A1. The HA-tagged rabbit A1 (WT), A1 mutated in the active site motif (E63A and E63Q) were used. (**D**) A1 proteins from small animal species are encapsidated into HIV-1 virions. The producer cells were collected and lyzed, while the released virus in the supernatants were collected by ultracentrifugation. The cells and virion lysates were then subjected to Western analysis using an antibody specific for the HA tag and HIV-1 Gag CA. The immunoblot probed with anti-β-actin antibody of the proteins present in the cell lysates is shown.

found to be packaged into HIV-1 virions, but variations in the efficiency of the incorporation of each A1 protein were seen. Rabbit A1 was incorporated efficiently, which could explain for its potent antiviral activity. The incorporations into HIV-1 virions of A1s from small animal species were not affected by expression of the Vif protein (Figure 2D). We therefore conclude that A1s like hA3G are specifically packaged into HIV-1 virions. However, unlike hA3G, this incorporation is not inhibited with coexpression of HIV-1 Vif. The mutant rabbit A1 E63A E63Q proteins were correctly expressed within the producer cells and also incorporated into the HIV-1 virions efficiently, as judged by western blot analysis (data not shown).

The HIV-1 Gag NC domain is required for A1 packaging

We next determined whether parts of Gag were dispensable for A1 packaging into virions, by use of previously described Gag mutants (22). Two Gag deletion mutants, δ10-110 mutant lacking residues 10 through 110, δ10-277 mutant lacking residues 10 through 277 or the Zwt-p6 mutant, in which NC is replaced by a leucine zipper from GCN4 were tested (Figure 3A). A1s from human, rabbit and rat as well as hA3G were efficiently incorporated into virus like particles (VLPs) formed by both Gag deletion δ10-110 and δ10-277 mutants (Figure 3B). Consistent with previous observations (22), hA3G was not incorporated into VLP formed by Zwt-p6 mutant. A1 from human and rabbit did not exhibit any detectable incorporation, while, A1 from rat caused a relatively small amount of incorporation into VLP formed by Zwt-p6 mutant (Figure 3B). Thus, almost all matrix and the amino-terminal two-thirds of capsid appear to be largely dispensable for A1 packaging, similar to those observed in hA3G packaging.

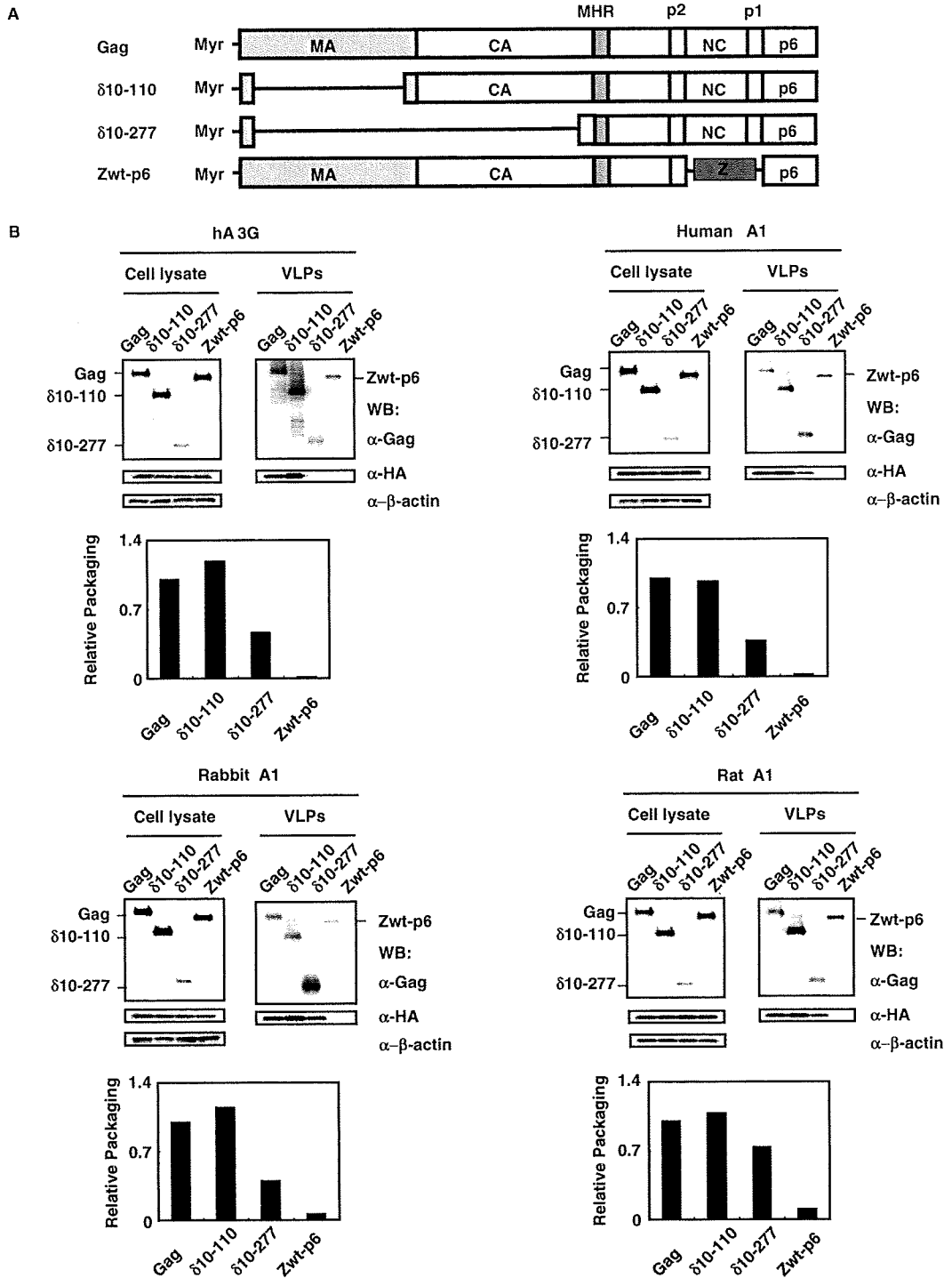

Figure 3. A1 proteins are encapsidated into HIV-1 virions via through the interaction with NC, but not the majority of Gag. (**A**) Schematic representation of the intact HIV-1 Gag precursor and its derivatives used in this study. The Gag are myristoylated (Myr-) on the N-tereminus of MA. The positions of the major homology region (MHR) and the various Gag cleavage sites are shown. (**B**) Western blot analysis of cell lysates and extracellular VLPs generated following transfection of 293T cells with plasmids expressing HIV-1 Gag or its derivatives shown in (A) and the HA-epitope tagged forms of the indicated APOBEC proteins. The producer cells were collected and lyzed, while the supernatants were harvested and released virus were collected by ultracentrifugation. The cells and virion lysates were then subjected to Western analysis using antibodies specific for the HIV-1 Gag CA and HA tag. The immunoblot probed with anti-β-actin antibody of the proteins present in the cell lysates is shown. Results were normalized to those obtained from the transfection of cells with the full-length Gag and APOBEC constructs, and were graphically shown as relative packaging.

Editing of HIV-1 proviral DNA and genomic RNA by A1 proteins

A3-mediated antiretroviral activity has been shown to be associated with cytidine deamination of nascently transcribed viral cDNAs following infection of target cells. Such dC-to-dU deamination in minus-strand DNA is detected as replacement of dG-to-dA in integrated proviral genomes. To address whether A1 functions in a similar manner, accumulation of dG-to-dA changes in the proviral DNA during reversetranscription was examined. Viral DNA was prepared from cells infected with wild-type or *Δvif* HIV-1 viruses produced in the presence of A1s from small animal species, and the 3′-end of the *pol* gene was analyzed for evidence of hypermutation. Consistent with previous reports, significant dG-to-dA hypermutation was observed for hA3G serving as a control for these studies (Table 1) and no dG-to-dA mutation was observed when the virus was prepared in the absence of an APOBEC protein (data not shown). In contrast, the predominant mutations induced by rabbit A1 that exhibited the most prominent antiviral activity were dC-to-dT changes (22 and 14 events in 23 664 and 24 480 bases in wild-type and *Δvif* viruses, respectively), which could have arisen through deamination of unpaired plus-stranded cDNA or virion RNA. To address the latter possibility, cell-free virions were purified and the genomic RNA was converted to cDNA for *pol* gene analyses. As can be seen in Table 2, there was a clear accumulation of dC-to-dT (U in the template RNA) changes in the RNAs of HIV-1 produced in the presence of rabbit A1 (39 and 51 events in 9792 and 8976 bases in wild-type and *Δvif* viruses, respectively), a frequency that is 4- to 5-fold higher than those observed in DNA sequencing. Thus, HIV-1 genome RNA as well as reversetranscribed proviral DNA could be a substrate for A1-mediated deamination.

The preferential sites of hypermutations induced by rabbit A1 were also examined (Figure 4). Consistent with previous observations (23–26), hA3G prefers to edit dC (marked by an asterisk) in the viral target DNA sequence C/TCC*. In constrast, rabbit A1, similar to mouse A3 (27) and human A3F (13,28,29), show preference for TTC* (Figure 4A). These results suggest that rabbit A1 inhibits HIV-1 infection by a deamination-dependent mechanism through targeting of proviral DNA sequences that are different from hA3G. Sequence context of the cytidine in viral RNA sequences mutated by rabbit A1 showed a clear

Table 1. Sequence analysis of reverse transcribed second-strand proviral DNA in the presence of mammalian A1s

			A1													
	hA3G		Human		Rabbit		Rabbit E63A		Rabbit E63Q		Hamster		Mouse		Rat	
	wt	*Δvif*	wt	*Δvif*	wt	*Δvif*	wt	*Δvif*	wt	*Δvif*	wt	*Δvif*	wt	*Δvif*	wt	*Δvif*
Clones sequenced	34	36	24	24	58	60	24	23	24	23	34	36	24	24	24	24
Total base pair sequenced	13 872	14 688	9792	9792	23 664	24 480	9792	9384	9792	9384	13 872	14 688	9792	9792	9792	9792
Clones with G to A	15	22	2	1	13	24	0	0	0	2	1	1	0	6	0	0
Number of G to A mutations	71	318	5	7	69	118	0	0	0	2	1	1	0	24	0	0
Number of G to A mutations per 1 kb	5.12	21.65	0.51	0.71	2.92	4.82	0	0	0	0.21	0.07	0.07	0	2.45	0	0
Clones with C to T	0	0	0	0	20	10	1	0	1	0	3	3	0	5	6	6
Number of C to T mutations	0	0	0	0	22	14	2	0	1	0	3	4	0	5	7	7
Number of C to T mutations per 1 kb	0	0	0	0	0.93	0.57	0.20	0	0.10	0	0.22	0.27	0	0.51	0.71	0.71
Number of Other mutations	0	1	0	0	1	3	0	0	0	0	0	0	0	0	0	0

A 408 bp fragment of HIV-1 *pol* region was amplified from reverse transcripts infected with wt or *Δvif* NL-Luc viruses produced in the presence of hA3G or mammalian A1s. The number in the clones of each group are shown (wt, wild-type). All mutations are designated using the conventional plus-strand nomenclature.

Table 2. Sequence analysis of HIV-1 genomic RNA in the presence of mammalian A1s

					A1							
	Mock		hA3G		Rabbit		Rabbit E63A		Rabbit E63Q		Rat	
	wt	*Δvif*	wt	*Δvif*	wt	*Δvif*	wt	*Δvif*	wt	*Δvif*	wt	*Δvif*
Clones sequenced	23	23	21	24	24	22	21	23	24	24	22	24
Total base pair sequenced	9384	9384	8568	9792	9792	8976	8568	9384	9792	9792	8976	9792
Clones with C to T	0	0	0	0	15	17	0	0	0	0	6	13
Number of C to T mutations	0	0	0	0	39	51	0	0	0	0	13	17
Number of C to T mutations per 1 kb	0	0	0	0	3.98	5.68	0	0	0	0	1.45	1.74
Number of Other mutations	0	2	1	0	1	0	0	1	1	0	0	0

This experiment was performed as described in the legend for Table 1, except that the genomic RNA of HIV-1 was amplified (wt, wild-type).

A hA3G

	−2	−1	C	1	2
A	18.3%	1.4%	0.0%	28.2%	33.8%
C	**40.8%**	**87.3%**	**100.0%**	33.8%	18.3%
G	0.0%	0.0%	0.0%	2.8%	11.3%
T	**40.8%**	11.3%	0.0%	**35.2%**	**36.6%**
	C/T	**C**	**C**	**T**	**T**

	−2	−1	C	1	2
A	20.4%	0.9%	0.0%	23.9%	**43.1%**
C	23.6%	**80.5%**	**100.0%**	29.2%	20.4%
G	0.3%	0.0%	0.0%	0.6%	6.0%
T	**55.7%**	17.9%	0.0%	**46.2%**	30.5%
	T	**C**	**C**	**T**	**A**

Rabbit A1

	−2	−1	C	1	2
A	34.8%	0.0%	0.0%	24.6%	27.5%
C	13.0%	2.9%	**100.0%**	20.3%	2.9%
G	11.6%	0.0%	0.0%	2.9%	5.8%
T	**40.6%**	**97.1%**	0.0%	**52.2%**	**63.8%**
	T	**T**	**C**	**T**	**T**

NL-luc wt

	−2	−1	C	1	2
A	28.0%	0.0%	0.0%	22.0%	38.1%
C	19.5%	14.4%	**100.0%**	37.3%	12.7%
G	0.0%	0.0%	0.0%	1.7%	6.8%
T	**52.5%**	**85.6%**	0.0%	**39.0%**	**42.4%**
	T	**T**	**C**	**T**	**T**

NL-luc Δvif

B Rabbit A1

	−2	−1	C	1	2
A	30.8%	41.0%	0.0%	**51.3%**	12.8%
C	**35.9%**	0.0%	**100.0%**	10.3%	20.5%
G	15.4%	0.0%	0.0%	5.1%	28.2%
T	17.9%	**59.0%**	0.0%	33.3%	**38.5%**
	C	**A/T**	**C**	**A/T**	**T**

NL-lucwt RNA

	−2	−1	C	1	2
A	31.4%	35.3%	0.0%	**54.9%**	19.6%
C	**47.1%**	0.0%	**100.0%**	0.0%	11.8%
G	9.8%	0.0%	0.0%	0.0%	**35.3%**
T	11.8%	**64.7%**	0.0%	45.1%	33.3%
	C	**A/T**	**C**	**A/T**	**G**

NL-luc ΔvifRNA

Figure 4. Comparison of the preferred sequence context for cytidine deamination by rabbit A1 in first strand cDNA and the genomic RNA of wild-type or*Δvif* viruses. (**A**) TTC*T in the HIV-1 minus-strand cDNA was the preferred tetranucleotide target of rabbit A1. Shown are percentages of each nucleotide found at the −2, −1, +1 and +2 positions relative to the dC residue targeted for deamination (position zero). The consensus DNA sequence is shown at the bottom of each minitable by bold. (**B**) WC*W sequence in the HIV-1 genome was the preferred RNA target of rabbit A1. Comparison of the preferred sequence observed in the viral genomic RNA produced in the presence of rabbit A1. All of the mutations in HIV-1 genomic RNA aligned with respect to the cytidine (**C**) targeted for deamination (position zero). The frequency with which each of the four bases found at positions adjacent to the deaminated C is indicated. The consensus RNA sequence is shown at the bottom of each minitable by bold.

WCW (W is A or T) trinucleotide preference on both the wild-type and *Δvif* HIV-1 genomic RNA (Figure 4B). The cytosine residue within WCW sequences was reported to be highly conserved as the apoB mRNA-editing site sequence by A1 protein among divergent of mammalian species (30). Rabbit A1 deaminated the cytosines in the genomic RNA but with different frequencies; some cytosines were changed at high frequencies, whereas others were not changed in any of the clones (Figure S4). Taken together, analysis of these mutations confirms that the inhibitory effects observed in rabbit A1s were based on, at least in part, cytosine-deaminating activity on viral genomic RNA, and the analysis of mutational hot spots indicated that the molecular mechanisms for editing of HIV-1 genome RNA and apoB mRNA overlap.

A1s from small animal species exhibit broad antilentiviral activity

To assess the breath of A1-mediated antiviral activity, the activities of these proteins on SIV infectivity were examined. A single-round assay was used to measure the infectivity of wild-type and *Δvif* SIVmac, and SIVagm luciferase reporter viruses (5), in the presence of A1s. VSV-G pseudotyped viral supernatants were collected, normalized for SIV CA p27 and used to infect 293T cells. As expected, hA3G caused a profound decrease in infectivity of both wild-type and *Δvif* SIV viruses (Figure 5A and C). A1 from rodents were found to be moderately active, but rabbit A1 significantly (>100-fold) reduced the infectivity of wild-type and *Δvif* SIV viruses. In contrast to A1 from small animal species, A1 from human intestine showed no antiviral activity. Expression of catalytic site mutant forms of rabbit A1 (E63A, E63Q) has little effect on the infectivity of SIV (Figure 5B and D), suggesting that the deaminase activity is also important for SIV repressive activities.

To measure the activities of A1 proteins on FIV infectivity, plasmids expressing APOBECs were cotransfected with an FIV (pFIV-H1/U6-copGFP) genome along with the packaging pFIV-34N plasmid and pVSV-G.

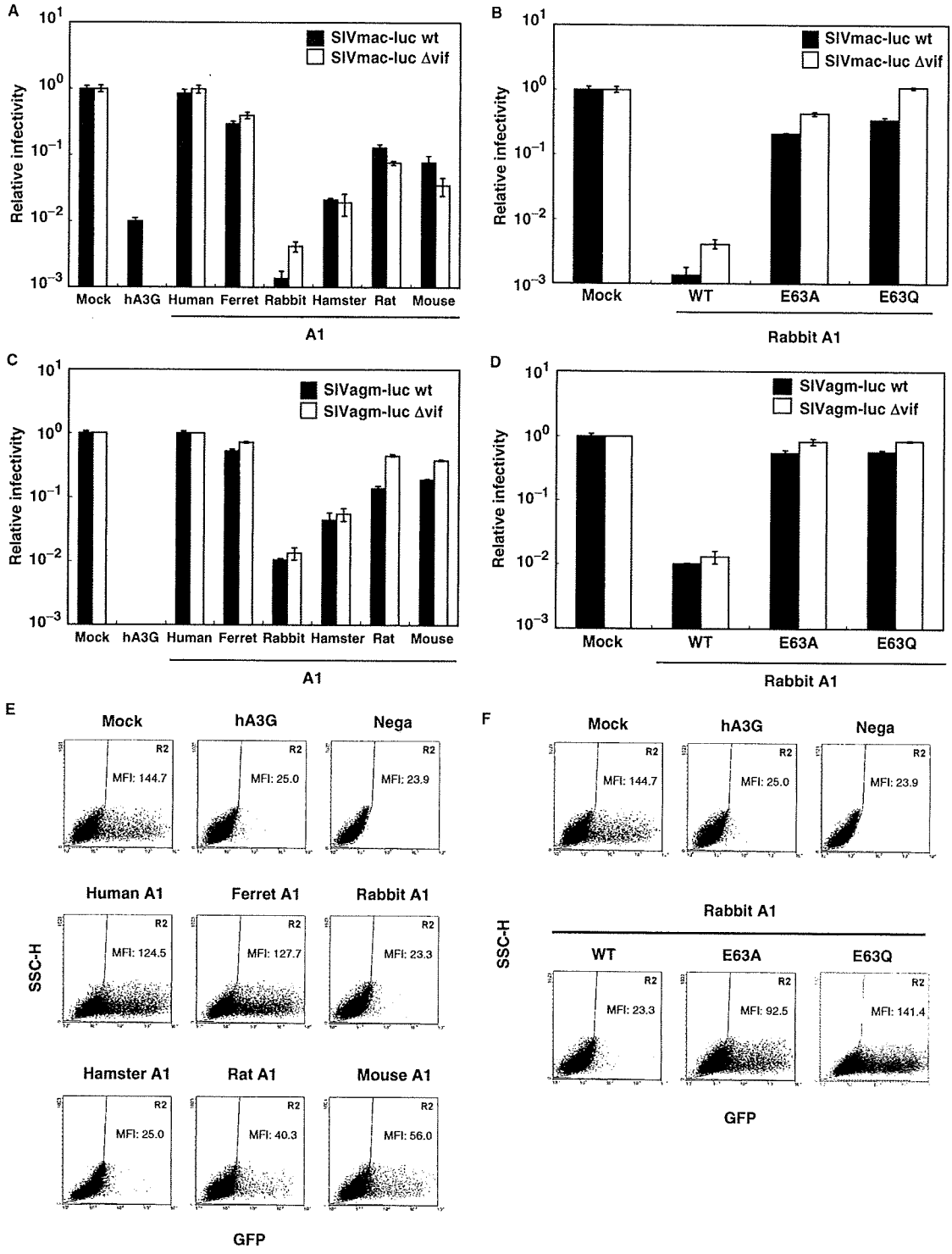

Figure 5. Inhibition of SIV and FIV infection by A1s. Wild-type and *Δvif* SIVmac (**A** and **B**), wild-type and *Δvif* SIVagm (**C** and **D**) luciferase reporter viruses pseudotyped were prepared. 293T cells were transfected with 1.5 μg of luciferase reporter viruses, 1.0 μg of pVSV-G and 0.5 μg of HA-tagged APOBECs (A and C) or rabbit A1 with catalytic site mutations (B and D). Virus-containing supernatants were normalized for equal p27 content and used for the infection. At 48 h postinoculation, virus-induced luciferase activity was measured and presented as described. VSV-G pseudotyped FIV GFP reporter viruses were produced in 293T cells transfected with 1.5 μg of pFIV-H1/copGFP and pFIV-34N, 1.0 μg of pVSV-G and 0.5 μg of HA-tagged APOBECs (**E**) or rabbit A1 with catalytic active site mutations (**F**). At 48 h postinoculation with FIV-GFP virions normalized for equal RT activity, cells exhibiting GFP fluorescence of target 293T cells were analyzed on flow cytometry. The level of GFP MFI detected within the GFP-positive windows are indicated. Comparable results were obtained in three additional experiments.

Viral supernatants of pseudotyped virions were collected, normalized for RT activity and used to infect 293T cells. The GFP expression was analyzed by flow cytometry at 48 h postinfection. Large proportion of of 293T cells were positive for GFP expression, with a MFI of 144.7, while in the cells transduced with hA3G containing FIV virions, only a few green cells were present, with 5.7-fold lower MFI of 25.0 (Figure 5E). Interestingly, similar to primate lentiviruses, the infectivity of FIV was significantly reduced in the presence of rabbit A1, with a 6.2-fold lower MFI of 23.3. We also detected reduced GFP signals in the cells transduced with rodent A1-containing virions, while human and ferret A1s caused minimal reduction in the number of GFP positive cells (Figure 5E). As seen in Figure 5F, rabbit A1 with catalytic site mutation E63A caused a slight decrease in FIV infectivity, but the E63Q mutation had no effect. Thus, the results using HIV-1, SIVmac, SIVagm and FIV reporter viruses combined suggest that the A1s from small animal species have a relatively broad lentivirus restriction potential that is mainly mediated through deaminase-dependent mechanism.

A1s affect MLV virion infectivity

Evidence is mounting that some APOBEC proteins can target a variety of retroviral substrates, such as various oncovirus and spumavirus. The A3 orthologs from artiodactyls; cattle, pigs and sheep, as well as hAB and hA3G have been reported to exert antiviral activity on MLV (6,13,23,24). These findings suggest that A3s in artiodactyls could function as barriers of cross-subspecies transmission of MLV from mice. Interestingly, this simple oncovirus is resistant to the mouse A3, explaining the absence of a Vif-like activity in MLV (27,31), but the underlying mechanism is currently unknown (32). Therefore, we examined whether the A1s expressed in small animal species affect MLV infection. MLV-based reporter viruses were produced by transient transfection of pFB-Luc, encoding the luciferase gene, into the MLV packaging cell line GP293 with pVSV-G, in the presence of APOBEC proteins. As shown in Figure 6A, hA3G was able to restrict the infectivity of MLV, consistent with previous reports (13,23,24). Interestingly, MLV infectivity was inhibited ~7-fold by rabbit A1, while A1s from other mammalian species had none or only moderate effect. Similar results were obtained with another murine retroviral vector, pFB-hrGFP (data not shown). Deaminase-defective rabbit A1s retained only partial antiviral activity (Figure 6B) despite comparable levels of MLV virion incorporation (Figure 6C). These data suggest that A1 from small animal species functions as potential barriers of cross-species transmission of this gammmaretroviruses from mice.

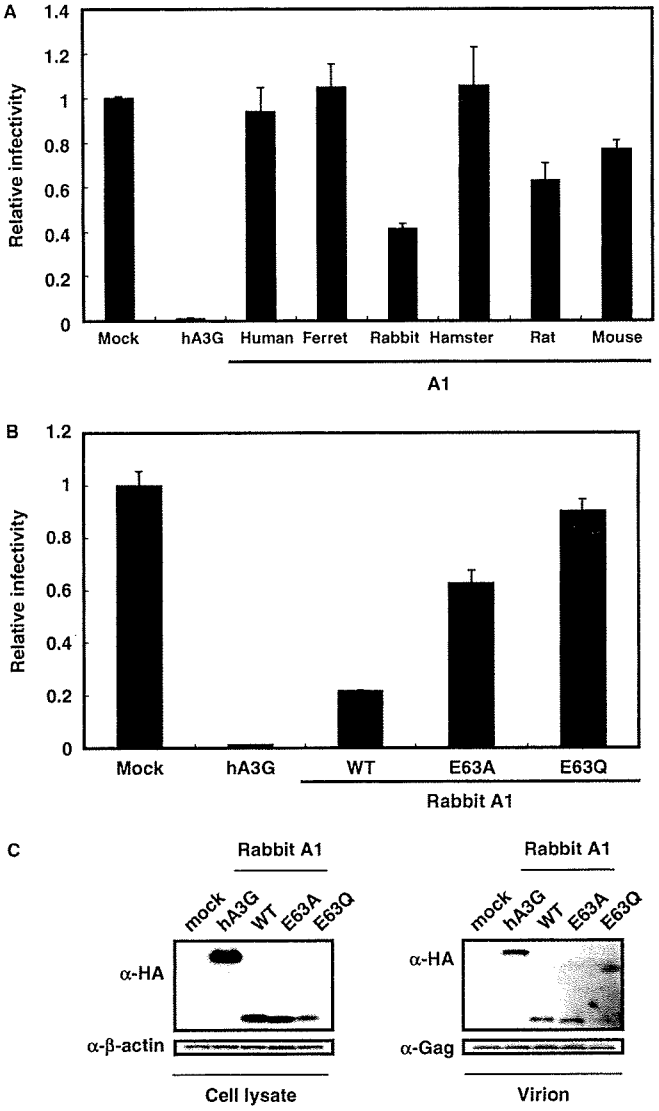

Figure 6. Inhibition of MLV infection by A1s. (**A** and **B**) MLV packaging cell line GP293 were transfected with 1.5 μg of luciferase pFB-Luc reporter plasmids, 1.0 μg of pVSV-G and 0.5 μg of HA-tagged APOBECs or rabbit A1 with catalytic site mutations. Virus-containing supernatants were normalized for equal MLV p30 CA content and used for the infection of the MDTF cells. Virus-induced intracellular luciferase activity was measured and presented as described. (**C**) Rabbit A1 proteins are encapsidated into MLV virions. After transfection, released virion was collected by ultracentrifugation, while the producer cells were collected and lyzed. The cells and virion lysates were then subjected to Western analysis using antibodies specific for the HA tag and MLV Gag CA. An immunoblot probed with anti-β-actin antibody of the proteins present in the cell lysates is also shown. While only the immunoblot of p30 CA performed with the disrupted virions is presented, closely similar results were also obtained using the cell lysates (data not shown).

DISCUSSION

In this study, we showed that single domain cytidine deaminase A1 from rodents (mouse, rat and hamster) and largomorphs (rabbit) are capable of inhibiting the infectivity of various lentiviruses in tissue culture models. A rank order in anti-HIV potency was seen, with rabbit A1 showing the greatest activity. The finding of more efficient virion incorporation of rabbit as compared to other small animal species A1 proteins may be a contributing factor. Catalytic site mutant analysis suggested a deaminase-dependent restriction mechanism, with genomic RNA as well as reversetranscribed proviral DNA serving as substrates for A1-mediated deamination.

A clear accumulation of C-T changes in the genomic RNAs of HIV-1 produced in the presence of rabbit A1 was observed, with G-A changes in the proviral DNA. Furthermore, expression of catalytic site mutant forms of rabbit A1 has little effect on the viral infectivity, supporting the importance of the deaminase activity for these repressive activities. Cytidine deaminase-defective A3 mutants have been shown to exhibit significant antiviral activity (33), implying that antiviral and deaminase activities can be uncoupled. Further evidence in support of editing-independent antiviral mechanism comes from studies on the enzymatically inactive, high-molecular mass complex of hA3G (34) as well as on the antiviral activity against hepatitis B virus (HBV) (35). Nevertheless, more recent studies using deaminase-defective A3 mutants show that efficient inhibition of HIV-1 or retroelements requires catalytically active A3 (36,37). In this regard, although deaminase-defective rabbit A1 mutants were shown to inhibit various lentivirus and MLV, these antiviral activities were significantly lower than those seen with wild-type A1. The suppressive activity of A1, therefore, is principally associated with its cytidine deaminase activity.

We demonstrated that the molecular mechanism for A1 editing of the HIV-1 genomic RNA and apoB mRNA overlapped. The C to U editing of apoB mRNA is shown to be a nuclear event (38), mediated by a complex composed of A1 homodimer and an A1 complementation factor (ACF) (39–41). Expression of ACF mRNA in cells such as Caco-2, a human colon cancer-derived cell line demonstrated to edit endogenous apoB mRNA has been documented (42). However, mRNA for ACF could not be detected by RT-PCR in 293T cells used for retorovirus production in this study (Supplementary Figure S5). Thus, the site(s) in virus-producing cells (e.g. nucleus, cytoplasm or both) where the deamination of HIV-1 genomic RNA takes place remains to be identified, and further experiments are needed to fully understand the role of ACF in the editing of retroviral genome observed in the present study.

In our study, A1s were expressed using both a chick β-actin (CAG) and a cytomegalovirus promoter-driven expression vector, and the concentration of A1s required to mediate antiviral activity was titrated carefully. We found that only 0.05 μg of rabbit A1 was required to achieve significant inhibition against HIV-1 (Figure 2B). Moreover, the antiviral activity of rabbit A1 appeared to be more potent than hA3G (Supplementary Figure S1), and this is unlikely to be explained by differences in virion incorporation of the two enzymes (Figure 2D). Taken together, the data suggest that antiretroviral activities of A1s observed in this study were not solely due to using overexpressed protein systems.

We found that human A1 exhibited no antiretroviral activity, consistent with reports of others (12,13,29,43). A1 from hominoids, therefore, appears to exclusively mediate the C to U editing of apoB mRNA, giving rise to two proteins with different sizes in the gastrointesitinal tissues that function in lipid transport and metabolism. As there have been no reports thus far of lentivirus infection in rodents, the antiviral activity of A1 proteins in rodents seen against HIV, SIV and FIV are also unlikely to have evolved originally to restrict infection of these lentiviruses. Nevertheless, the finding that rabbit A1 can restrict MLV raises the possibility that A1s from small animals species evolved to restrict cross-subspecies transmission of oncoviruses from mice. Furthermore, endogenous lentivirus of rabbits has recently been described (44), lending biological significance to the antilentiviral activity in lagomorphs reported here. Further studies of the antiviral activities of A1 proteins from other members of the placentalia super-order of Laurasiatheria; cetartiodactyla (cow, pig, sheep) and carnivore (cat) will be required to fully understand the complex evolutionary history of *APOBEC* genes as an intrinsic resistance mechanism against retroelements.

HIV-1 exhibits a highly restricted host cell tropism. The identification of chemokine receptors as entry cofactors with human CD4 raises the possibility that small animal species, in particular, rodents could be engineered to express these molecules, thereby rendering them able to support a productive HIV-1 infection. However, HIV-1 replication in rodents (45–47) and rabbits (48,49) expressing human versions of the HIV-1 receptors appeared to be limited and variable. Our findings with A1 suggest that this enzyme may be partly responsible for the inefficient replication of HIV-1 observed in rabbit as well as rodent cells. Blocking of antiviral A1 function by RNA interference in cells from small animal species should verify whether A1 acts as an intrinsic resistance factor. Further understanding of these species-nonspecific repressive activities to HIV-1 replication at the late phase, in conjugation with the early block owing to the different classes of activities, such as TRIM5α (50,51), may suggest approaches to the development of small animal models of HIV-1 infection.

SUPPLEMENTARY DATA

Supplementary Data are available at NAR Online.

ACKNOWLEDGEMENTS

We thank C. Cheng-Mayer for critical reviewing the article. We also thank P. D. Bieniasz, N. Landau, D. Trono, M. Hayami and H. Amanuma for providing reagents; J. Shibata, K. Monde and K. Yusa for discussions.

FUNDING

Higo Bank; Grants from the Japan Health Science foundation, Ministry of Health and Welfare of Japan; The Cooperative Research Project on Clinical and Epidemiological Studies of Emerging and Re-emerging Infectious Diseases; Research and Education Program for Development of Therapy of Emerging and Reemerging Infectious Diseases Including AIDS. Funding for open access charge: Higo Bank.

Conflict of interest statement. None declared.

REFERENCES

1. Bieniasz,P.D. (2004) Intrinsic immunity: a front-line defense against viral attack. *Nat. Immunol.*, **5**, 1109–1115.
2. Holmes,R.K., Malim,M.H. and Bishop,K.N. (2007) APOBEC-mediated viral restriction: not simply editing? *Trends Biochem. Sci.*, **32**, 118–128.
3. Chiu,Y.L. and Green,W.C. (2008) The APOBEC3 cytidine deaminases: an innate defensive network opposing exogenous retroviruses and endogenous retroelements. *Annu. Rev. Immunol.*, **26**, 317–353.
4. Sheehy,A.M., Gaddis,N.C., Choi,J.D. and Malim,M.H. (2002) Isolation of a human gene that inhibits HIV-1 infection and is suppressed by the viral Vif protein. *Nature*, **418**, 646–650.
5. Mariani,R., Chen,D., Schrofelbauer,B., Navarro,F., Konig,R., Bollman,B., Munk,C., Nymark-McMahon,H. and Landau,N.R. (2003) Species-specific exclusion of APOBEC3G from HIV-1 virions by Vif. *Cell*, **114**, 21–31.
6. Jonsson,S.R., Hache,G., Stenglein,M.D., Fahrenkrug,S.C., Andresdottir,V. and Harris,R.S. (2006) Evolutionarily conserved and non-conserved retrovirus restriction activities of artiodactyl APOBEC3F proteins. *Nucleic Acids Res.*, **34**, 5683–5694.
7. Munk,C., Zielonka,J., Constabel,H., Kloke,B.P., Rengstl,B., Battenberg,M., Bonci,F., Pistello,M., Lochelt,M. and Cichutek,K. (2007) Multiple restrictions of human immunodeficiency virus in feline cells. *J. Virol.*, **81**, 7048–7060.
8. Munk,C., Beck,T., Zielonka,J., Hotz-Wagenblatt,A., Chareza,S., Battenberg,M., Thielebein,J., Cichutek,K., Bravo,I.G., O'Brien,S.J. *et al.* (2008) Functions, structure, and read-through alternative splicing of feline APOBEC3 genes. *Genome Biol.*, **9**, R48.
9. Chester,A., Scott,J., Anant,S. and Navaratnam,N. (2000) RNA editing: cytidine to uridine conversion in apolipoprotein B mRNA. *Biochem. Biophys. Acta.*, **1494**, 1–13.
10. Keegan,L.P., Gallo,A. and O'Connell,M.A. (2001) The many roles of an RNA editor. *Nat. Rev. Genet.*, **2**, 869–878.
11. Harris,R.S., Petersen-Mahrt,S.K. and Neuberger,M.S. (2002) RNA editing enzyme APOBEC1 and some of its homologs can act as DNA mutators. *Mol. Cell*, **10**, 1247–1253.
12. Bishop,K.N., Holmes,R.K., Sheehy,A.M. and Malim,M.H. (2004) APOBEC-mediated editing of viral RNA. *Science*, **305**, 645.
13. Bishop,K.N., Holmes,R.K., Sheehy,A.M., Davidson,N.O., Cho,S.-J. and M. H. Malim. (2004) Cytidine deamination of retroviral DNA by diverse APOBEC proteins. *Curr. Biol.*, **14**, 1392–1396.
14. Niwa,H., Yamamura,K. and Miyazaki,J. (1991) Efficient selection for high-expression transfectants with a novel eukaryotic vector. *Gene*, **108**, 193–199.
15. Ohsugi,T. and Koito,A. (2007) Human T cell leukemia virus type I is resistant to the antiviral effects of APOBEC3. *J. Virol. Methods*, **139**, 93–96.
16. Koito,A., Kameyama,Y., Cheng-Mayer,C. and Matsushita,S. (2003) Susceptibility of mink (*Mustera vision*)-derived cells to replication by human immunodeficiency virus type 1. *J. Virol.*, **77**, 5109–5117.
17. Burns,J.C., Friedmann,T., Driever,W., Burrascano,M. and Yee,J.-K. (1993) Vesicular stomatitis virus G glycoprotein pseudotyped retroviral vectors: concentration to very high titer and efficient gene transfer into mammalian and nonmammalian cells. *Proc. Natl Acad. Sci. USA*, **90**, 8033–8037.
18. Koito,A., Hattori,T., Matsushita,S., Maeda,Y., Nozaki,C., Sagawa,K. and Takatsuki,K. (1988) . Conserved immunogenic region of a major core protein (p24) of human and simian immunodeficiency viruses. *AIDS Res. Hum. Retroviruses*, **4**, 409–417.
19. Yamanaka,S., Poksay,K.S., Balestra,M.E., Zeng,G.-Q. and Innerarity,T.L. (1994) Cloning and mutagenesis of the rabbit apoB mRNA editing protein. A zinc motif is essential for catalytic activity, and noncatalytic auxiliary factor(s) of the editing complex are widely distributed. *J. Biol. Chem.*, **269**, 21725–21734.
20. Harris,R.S. and Liddament,M.T. (2004) Retroviral restriction by APOBEC proteins. *Nat. Rev. Immunol.*, **4**, 868–877.
21. Betts,L., Xiang,S., Short,S.A., Wolfenden,R. and Carter,C.W.J. (1994) Cytidine deaminase. The 2.3 A crystal structure of an enzyme: transition-state analog complex. *J. Mol. Biol.*, **235**, 635–656.
22. Zennou,V., Perez-Caballero,D., Gottlinger,H. and Bieniasz,P.D. (2004) APOBEC3G incorporation into human immunodeficiency virus type 1 particles. *J. Virol.*, **78**, 12058–12061.
23. Harris,R.S., Bishop,K.N., Sheehy,A.M., Craig,H.M., Petersen-Mahrt,S.K., Watt,I.N., Neuberger,M.S. and Malim,M.H. (2003) DNA deamination mediates innate immunity to retroviral infection. *Cell*, **113**, 803–809.
24. Mangeat,B., Turelli,P., Caron,G., Friedli,M., Perrin,L. and Trono,D. (2003) Broad antiretroviral defence by human APOBEC3G through lethal editing of nascent reverse transcript. *Nature*, **424**, 99–103.
25. Zhang,H., Yang,B., Pomerantz,R.J., Zhang,C., Arunachalam,S.C. and Gao,L. (2003) The cytidine deaminase CEM15 induces hypermutation in newly synthesized HIV-1 DNA. *Nature*, **424**, 94–98.
26. Yu,Q., Konig,R., Pillai,S., Chiles,K., Kearney,M., Palmer,S., Richman,D., Coffin,J.M. and Landau,N.R. (2004) Single-strand specificity of APOBEC3G accounts for minus-strand deamination of the HIV genome. *Nat. Struct. Mol. Biol.*, **11**, 435–442.
27. Kobayashi,M., Takaori-Kondo,A., Shindo,K., Abudu,A., Fukunaga,K. and Uchiyama,T. (2004) APOBEC3G targets specific virus species. *J. Virol.*, **78**, 8238–8244.
28. Liddament,M.T., Brown,W.L., Schumacher,A.J. and Harris,R.S. (2004) APOBEC3F properties and hypermutation preferences indicate activity against HIV-1 in vivo. *Curr. Biol.*, **14**, 1385–1391.
29. Wiegand,H.L., Doehle,B.P., Bogerd,H.P. and Cullen,B.R. (2004) A second human antiretroviral factor, APOBEC3F, is suppressed by the HIV-1 and HIV-2 Vif proteins. *EMBO J.*, **23**, 2451–2458.
30. Fujino,T., Navaratnam,N., Jarmuz,A., Von Haeseler,A. and Scott,J. (1999) C – U editing of apolipoprotein B mRNA in marsupials: identification and characterization of APOBEC-1 from the American opossum *Monodelphus domestica*. *Nucleic Acids Res.*, **27**, 2662–2671.
31. Doehle,B.P., Schafer,A., Wiegand,H.L., Bogerd,H.P. and Cullen,B.R. (2005) Differential sensitivity of murine leukemia virus to APOBEC3-mediated inhibition is governed by virion exclusion. *J. Virol.*, **79**, 8201–8207.
32. Browne,E.P. and Littman,D.R. (2008) Species specific restriction of Apobec3, mediated hypermutation. *J. Virol.*, **82**, 1305–1313.
33. Newman,E.N., Holmes,R.K., Craig,H.M., Klein,K.C., Lingappa,J.R., Malim,M.H. and Sheehy,A.M. (2005) Antiviral function of APOBEC3G can be dissociated from cytidine deaminase activity. *Curr. Biol.*, **15**, 166–170.
34. Chiu,Y.-L., Soros,V.B., Kreisberg,J.F., Stopak,K., Yonemoto,W. and Greene,W.C. (2005) Cellular APOBEC3G restricts HIV-1 infection in restricting CD4+ T cells. *Nature*, **435**, 108–114.
35. Turelli,P., Mangeat,B., Jost,S.S., Vianin,S. and Trono,D. (2004) Inhibition of hepatitis B virus replication by APOBEC3G. *Science*, **303**, 1829.
36. Miyagi,E., Opi,S., Takeuchi,H., Khan,M., Goila-Gaur,R., Kao,S. and Strebel,K. (2007) Enzymatically active APOBEC3G is required for efficient inhibition of human immunodeficiency virus type 1. *J. Virol.*, **81**, 13346–13353.
37. Schumacher,A.J., Hache,G., MacDuff,D.A., Brown,W.L. and Harris,R.S. (2008) The DNA deaminase activity of human APOBEC3G is required for Ty1, MusD and human immunodeficiency virus type 1 restriction. *J. Virol.*, **82**, 2652–2660.
38. Lau,P.P., Xiong,W.J., Zhu,H.J., Chen,S.H. and Chan,L. (1991) Apolipoprotein B mRNA editing is an intranuclear event that occurs posttranscriptionally coincident with splicing and polyadenylation. *J. Biol. Chem.*, **266**, 20550–20554.
39. Lellek,H., Kirsten,R., Diehl,L., Apostel,F., Buck,F. and Greeve,J. (2000) Purification and molecular cloning of a novel essential component of the apolipoprotein B mRNA editing enzyme-complex. *J. Biol. Chem.*, **275**, 19848–19856.
40. Mehta,A., Kinter,M.T., Sherman,N.E. and Driscoll,D.M. (2000) Molecular cloning of apobec-1 complementation factor, a novel RNA-binding protein involved in the editing of apolipoprotein B mRNA. *Mol. Cell. Biol.*, **20**, 1846–1854.
41. Chester,A., Somasekaram,A., Tzimina,M., Jarmuz,A., Gisbourne,J., O'Keefe,R., Scott,J. and Navaratnam,N. (2003) The apolipoprotein B mRNA editing complex performs a multifunctional cycle and suppresses nonsense-mediated decay. *EMBO J.*, **22**, 3971–3982.

42. Jiao,S., Moberly,J.B. and Schonfeld,G. (1990) Editing of apolipoprotein B messenger RNA in differentiated Caco-2 cells. *J. Lipid Res.*, **31**, 695–700.
43. Zheng,Y.-H., Irwin,D., Kurosu,T., Tokunaga,K., Sata,T. and Peterlin,B.M. (2004) Human APOBEC3F is another host factor that blocks human immunodeficiency virus type 1 replication. *J. Virol.*, **78**, 6073–6076.
44. Katzourakis,A., Tristem,M., Pybus,O.G. and Gifford,R.J. (2007) Discovery and analysis of the first endogenous lentivirus. *Proc. Natl Acad. Sci. USA*, **104**, 6261–6265.
45. Browning,J., Horner,J.W., Pettoello-Mantovani,M., Raker,C., Yurasov,S., DePinho,R.A. and Goldstein,H. (1997) Mice transgenic for human CD4 and CCR5 are susceptible to HIV infection. *Proc. Natl Acad. Sci. USA*, **94**, 14637–14641.
46. Sawada,S., Gowrishankar,K., Kitamura,R., Suzuki,M., Suzuki,G., Tahara,S. and Koito,A. (1998) Disturbed $CD4^+$ T cell homeostasis and in vitro HIV-1 susceptibility in transgenic mice expressing T cell line-tropic HIV-1 receptors. *J. Exp. Med.*, **187**, 1439–1449.
47. Keppler,O.T., Welte,F.J., Ngo,T.A., Chin,P.A., Patton,K.S., Tsou,C.-L., Abbey,N.W., Sharkey,M.E., Grant,R.M., You,Y. *et al.* (2002) Progress toward a human CD4/CCR5 transgenic rat model for de novo infection by human immunodeficiency virus type 1. *J. Exp. Med.*, **195**, 719–736.
48. Dunn,C.S., Mehtali,M., Houdebine,L.M., Gut,J.-P., Kirn,A. and Aubertin,A.-M. (1995) Human immunodeficiency virus type 1 infection of human CD4-transgenic rabbits. *J. Gen. Virol.*, **76**, 1327–1336.
49. Speck,R.F., Penn,M.L., Wimmer,J., Esser,U., Hague,B.F., Kindt,T.J., Atchison,R.E. and Goldsmith,M.A. (1998) Rabbit cells expressing human CD4 and human CCR5 are highly permissive for human immunodeficiency virus type 1 infection. *J. Virol.*, **72**, 5728–5734.
50. Stremlau,M., Owens,C.M., Perron,M.J., Kiessling,M., Autissier,P. and Sodroski,J. (2004) The cytoplasmic body component TRIM5alpha restricts HIV-1 infection in old world monkeys. *Nature*, **427**, 848–853.
51. Schaller,T., Hue,S. and Towers,G.J. (2007) An active TRIM5 in rabbits indicates a common antiviral ancestor for mammalian TRIM5 proteins. *J. Virol.*, **81**, 11713–11721.

Bioorganic & Medicinal Chemistry Letters 20 (2010) 354–358

Contents lists available at ScienceDirect

Bioorganic & Medicinal Chemistry Letters

journal homepage: www.elsevier.com/locate/bmcl

CD4 mimics targeting the mechanism of HIV entry

Yuko Yamada [a], Chihiro Ochiai [a], Kazuhisa Yoshimura [b], Tomohiro Tanaka [a], Nami Ohashi [a], Tetsuo Narumi [a], Wataru Nomura [a], Shigeyoshi Harada [b], Shuzo Matsushita [b], Hirokazu Tamamura [a,*]

[a] Institute of Biomaterials and Bioengineering, Tokyo Medical and Dental University, Chiyoda-ku, Tokyo 101-0062, Japan
[b] Center for AIDS Research, Kumamoto University, Kumamoto 860-0811, Japan

ARTICLE INFO

Article history:
Received 19 September 2009
Revised 20 October 2009
Accepted 22 October 2009
Available online 4 November 2009

Keywords:
CD4 mimic
HIV entry
Synergistic effect
CXCR4

ABSTRACT

A structure–activity relationship study was conducted of several CD4 mimicking small molecules which block the interaction between HIV-1 gp120 and CD4. These CD4 mimics induce a conformational change in gp120, exposing its co-receptor-binding site. This induces a highly synergistic interaction in the use in combination with a co-receptor CXCR4 antagonist and reveals a pronounced effect on the dynamic supramolecular mechanism of HIV-1 entry.

Recently, remarkable success has attended the clinical treatment of HIV-infected and AIDS patients, with 'highly active antiretroviral therapy (HAART)'. This approach involves a combination of two or three agents from two categories: reverse transcriptase inhibitors and protease inhibitors.[1] In addition, the molecular mechanism involved in HIV-entry and -fusion into host cells has been described in detail.[2] The complex interactions of surface proteins on cellular and viral membranes, which are designated as a dynamic supramolecular mechanism of HIV entry, are reported to be crucial to the viral infection. In a first step, an HIV envelope protein, gp120 interacts with a cell surface protein, CD4, leading to a conformational change in gp120 followed by subsequent binding of gp120 to a co-receptor CCR5[3] or CXCR4.[4] CCR5 and CXCR4 are the major co-receptors for the entry of macrophage-tropic (R5-) and T cell line-tropic (X4-) HIV-1, respectively. The interaction of gp120 with CCR5 or CXCR4 triggers entry of another envelope protein, gp41 to the cell membrane and formation of a gp41 trimer-of-hairpins structure, which causes fusion of HIV/cell-membranes and completes the infection.

Informed by this mechanism, a fusion inhibitor, enfuvirtide (fuzeon, Trimers & Roche)[5] and a CCR5 antagonist, maraviroc (Pfizer)[6] in addition to an integrase inhibitor, raltegravir (Merck)[7] have been used clinically. However, serious problems with chemotherapy still persist, including the emergence of viral strains with multi-drug resistance (MDR), considerable adverse effects and high costs. Consequently, development of novel drugs possessing mechanisms of action different from those of the above inhibitors is currently required. We have previously developed selective CXCR4 antagonists[8] and fusion inhibitors.[9] Furthermore, *N*-(4-Bromophenyl)-*N*′-(2,2,6,6-tetramethylpiperidin-4-yl)-oxalamide (**1**) and *N*-(4-chlorophenyl)-*N*′-(2,2,6,6-tetramethylpiperidin-4-yl)-oxalamide (**2**) were previously found using chemical library screening to inhibit syncytium formation by other researchers.[10] **1** and **2** bind to gp120 with binding affinities of K_d = 2.2 μM and 3.7 μM, respectively, blocking the interaction of gp120 with CD4 in the first step of an HIV-1 entry. Thus, in the present study we focus on the development of CD4 mimics that can block the interaction between gp120 and CD4. We have investigated the effect of CD4 mimics on conformational changes of gp120 and on their use in combination use with a CXCR4 antagonist.

Initially, molecular modeling of compound **2** docked into gp120 was carried out using docking simulations performed by the FlexSIS module of SYBYL 7.1 (Tripos, St. Louis) (Fig. 1).[11] The atomic coordinates of the crystal structure of gp120 with soluble CD4 (sCD4) were retrieved from Protein Data Bank (PDB) (entry 1RZJ) (Fig. 1a) and it was observed that Phe^{43} and Arg^{59} of the CD4 have multiple contacts with Asp^{368}, Glu^{370} and Trp^{427} of gp120, which are all conserved residues. An inspection of the environment of compound **2** docked in gp120 revealed the presence of a large cavity around the *p*-position of the phenyl ring of compound **2**, which could interact with the viral surface protein gp120 (Fig. 1b and c). Several analogs of **2** with substituents on the phenyl ring were therefore synthesized.

All compounds except **12** were synthesized by previously published methods (Scheme 1).[10b,12,13] Aniline derivatives (**3**) were coupled with ethyl oxalyl chloride to yield the corresponding ethyl oxalamates **4**. Saponification of the above oxalamates to the corresponding free acids and the subsequent coupling with 4-ami-

* Corresponding author.
E-mail address: tamamura.mr@tmd.ac.jp (H. Tamamura).

0960-894X/$ - see front matter © 2009 Elsevier Ltd. All rights reserved.
doi:10.1016/j.bmcl.2009.10.098

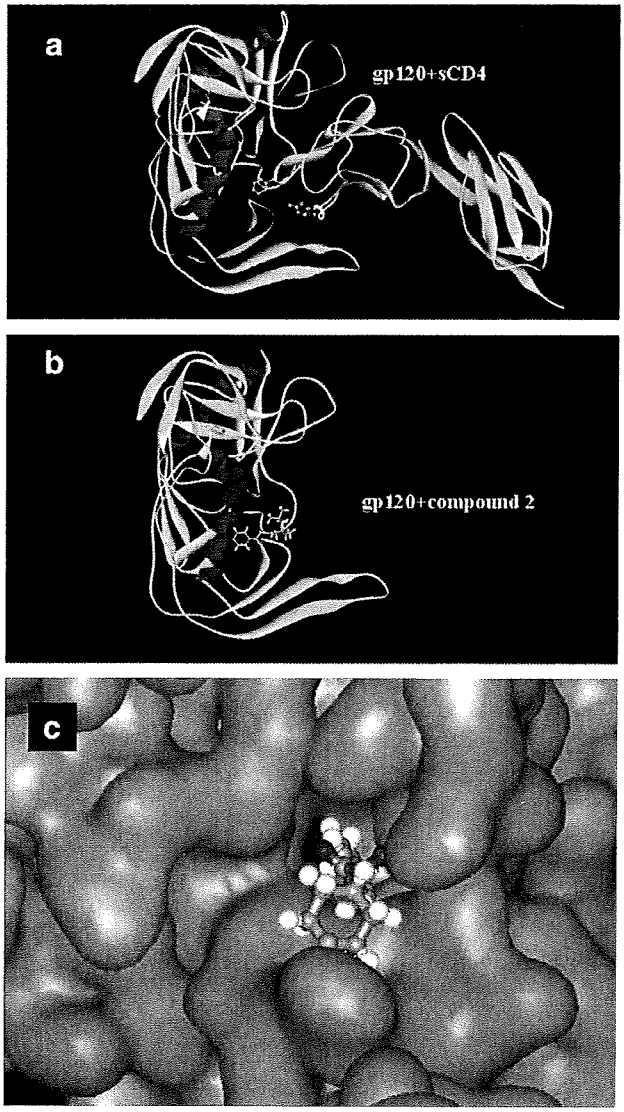

Figure 1. (a) The crystal structure of gp120 with soluble CD4 (sCD4) retrieved from the PDB (entry 1RZJ); (b) docking structure of compound **2** and gp120; (c) a focused figure of (b) shown by space-filling model.

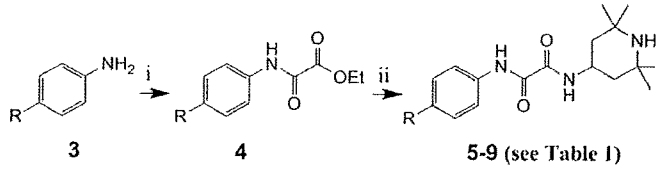

Scheme 1. Reagents and conditions: (i) ethyl oxalyl chloride, Et_3N; (ii) 1 M NaOH; 4-amino-2,2,6,6-tetramethylpiperidine, 1-(3-dimethylaminopropyl)-3-ethylcarbodiimide hydrochloride, 1-hydroxybenzotriazole, Et_3N.

no-2,2,6,6-tetramethylpiperidine using 1-ethyl-3-(3-dimethylaminopropyl)carbodiimide hydrochloride (EDC) and 1-hydroxybenzotriazole (HOBt) yielded compounds **5–9**. In the case of compound **12**, whose amide bond is not stable during the reaction of the saponification of the corresponding oxalamates, an alternative synthetic scheme was used (Scheme 2).[14] The reaction of *p*-nitroaniline (**10**) with oxalyl chloride gave the corresponding oxoacetamide **11**, which was subsequently coupled with 4-amino-2,2,6,6-tetramethylpiperidine to yield the desired compound **12**.

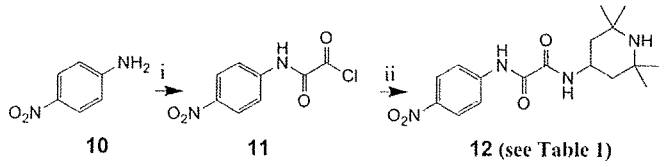

Scheme 2. Reagents and conditions: (i) oxalyl chloride, Et_3N; (ii) 4-amino-2,2,6,6-tetramethylpiperidine, Et_3N.

The anti-HIV activity of the synthetic compounds was evaluated against various viral strains including both laboratory and primary isolates (Table 1). IC_{50} values were determined by the 3-(4,5-dimethylthiazol-2-yl)-2,5-diphenyltetrazolium bromide (MTT) method[15] as the concentrations of the compounds which conferred 50% protection against HIV-1-induced cytopathogenicity in PM1/CCR5 cells. Cytotoxicity of the compounds based on the viability of mock-infected PM1/CCR5 cells was also evaluated using the MTT method. CC_{50} values were determined as the concentrations achieving 50% reduction of the viability of mock-infected cells. Compounds **1** and **2** showed potent anti-HIV activity against laboratory isolates, IIIB (X4, Sub B) and 89.6 (dual, Sub B) strains, and compound **2** also possessed potent activity against a primary isolate, an fTOI strain (R5, Sub B). All of the IC_{50} values were between 4 μM and 10 μM. Compound **1** was not tested against primary isolates. The potencies of compounds **1** and **2** are comparable to the reported binding affinities for gp120 (K_d = 2.2 and 3.7 μM, respectively).[10] Several of the new analogs of compounds **1** and **2** showed significant anti-HIV activity. Compound **5**, which has a phenyl group in place of the *p*-chlorophenyl group of compound **2**, did not show significant anti-HIV activity at concentrations below 100 μM against all strains tested except for an fTOI strain (R5, Sub B). This result suggests that a substituent at the *p*-position of the phenyl ring is critical for potent activity. Compound **6**, which has a fluorine atom at the *p*-position of the phenyl ring, showed moderate anti-HIV activity against laboratory isolates, IIIB (X4, Sub B) and 89.6 (dual, Sub B) strains (IC_{50} = 61 and 81 μM, respectively), but, at concentrations below 100 μM, failed to show significant anti-HIV activity against a primary isolate, a KYAG strain (R5, Sub B). Among halogen atoms, fluorine is less suitable than bromine or chlorine as a substituent at the *p*-position of the phenyl ring, as evidenced by compound **6**, which is 8–15-fold less potent than compounds **1** and **2** against IIIB (X4, Sub B) and 89.6 (dual, Sub B) strains. Compound **7**, which has a methyl group at the *p*-position of the phenyl ring, showed relatively more potent activity against IIIB (X4, Sub B) and 89.6 (dual, Sub B) strains (IC_{50} = 23 and 41 μM, respectively) than compound **6**. Compound **7** also showed significant anti-HIV activity against primary isolates, fTOI (R5, Sub B) and KYAG (R5, Sub B) strains (IC_{50} = 16 and 51 μM, respectively). Compound **8**, with a methoxy group at the *p*-position of the phenyl ring, did not show significant anti-HIV activity against all strains tested until a concentration of 100 μM was reached. In the biological assays, derivatives having electron-withdrawing substituents such as bromine, chlorine and fluorine at the *p*-position of the phenyl ring are relatively potent, whereas derivatives having electron-donating groups such as methoxy at this position are not potent. Furthermore, the steric effect of a substituent at the *p*-position of the phenyl ring appears to be critical to anti-HIV activity. The sum of Hammett constants (σ) of benzoic acid substituents[16] shown in Table 1 can be used to evaluate the electron-withdrawing or -donating effect of the substituents on the aromatic ring. The Taft E_s values[16a,17] were used as steric parameters for substituents at the *p*-position of the phenyl ring. The order of potency found for the halogen-containing derivatives in anti-HIV activity against laboratory isolates, IIIB (X4, Sub B) and 89.6 (dual, Sub B), is: compound **1** (R = Br) (σ = 0.23, E_s = −1.16), **2**

Table 1
Hammett constants (σ) and steric effects (E_s) of substituted aromatic rings and anti-HIV activity and cytotoxicity of synthetic compounds

Compd	R[a]	σ[b]	E_s[c]	IC_{50}[e] (μM)				CC_{50}[e] (μM)
				Lab. isolates		Primary isolates		
				IIIB (X4)	89.6 (dual)	fTOI (R5)	KYAG (R5)	
1	Br	0.23	−1.16	4	9	ND	ND	150
2	Cl	0.23	−0.97	8	10	5	>30	170
5	H	0	0	>100	>100	81	>100	350
6	F	0.06	−0.46	61	81	ND	>100	320
7	CH_3	−0.17	−1.24	23	41	16	51	210
8	OCH_3	−0.27	−0.55	>100	>100	ND	>100	340
9	CF_3	0.54	−2.40	ND	27	ND	ND	72
12	NO_2	0.78	−1.77[d]	ND	42	ND	ND	230
sCD4				0.010	0.021	0.0044	ND	ND

[a] See Schemes 1 and 2.
[b] σ = Hammett constant of a substitutent on a benzoic acid derivative.[16]
[c] E_s = steric effect of a substituent at the *para* position on the aromatic ring.[16a,17]
[d] The average value of −1.01 and −2.52, which are E_s values of the NO_2 group, −1.77, was used.
[e] Values are means of at least three experiments (ND = not determined).

(R = Cl) (σ = 0.23, E_s = −0.97), **6** (R = F) (σ = 0.06, E_s = −0.46) and **5** (R = H) (σ = 0, E_s = 0). This is the order of substituents' electron-withdrawing ability and also of their size. Methyl (σ = −0.17, E_s = −1.24) is an electron-donating group, but is almost as bulky as a bromine atom. Thus, the *p*-methyl derivative **7** has relatively potent anti-HIV activity against laboratory isolates, IIIB (X4, Sub B) and 89.6 (dual, Sub B), higher than that of compound **6** (R = F) but lower than that of compound **1** (R = Br) or **2** (R = Cl). The electron-donating ability of a methoxy group is stronger (σ = −0.27), but the bulk size is smaller (E_s = −0.55), than that of a methyl group. Thus, the *p*-methoxy derivative **8** has no significant anti-HIV activity against all strains tested at concentrations below 100 μM. Two derivatives containing bulkier and more potent electron-withdrawing substituents such as trifluoromethyl (R = CF_3) (σ = 0.54, E_s = −2.40) and nitro (R = NO_2) (σ = 0.78, E_s = −1.77) at the *p*-position of the phenyl ring were evaluated. Compounds **9** (R = CF_3) and **12** (R = NO_2) showed significant anti-HIV activity against an 89.6 (dual, Sub B) strain. These are less potent than compounds **1** and **2** and this is perhaps due to the excessive size of the substituents at the *p*-position. This suggests that a certain level of the bulk size and a potent electron-withdrawing ability of the substituents are preferable for anti-HIV activity. It is estimated that a cavity around the *p*-position of the phenyl ring of CD4 mimicking compounds would be optimally filled by bromine (E_s = −1.16) or a methyl group (E_s = −1.24) at *p*-position, and that an electron-deficient aromatic ring might interact tightly with a negatively charged group such as carboxy of Glu^{370}. In isothermal titration calorimetry (ITC) experiments reported elsewhere,[10c] compound **5** (R = H) does not have significant affinity for gp120, and compound **6** (R = F) has less potent affinity for gp120 than compound **2**, consistent with the present data. In all but one of the compounds, no significant cytotoxicity was detected (CC_{50} >150 μM, Table 1), the exception being compound **9** (R = CF_3) (CC_{50} = 72 μM). Compounds **7** and **12** have relatively low cytotoxicities, compared to compounds **1** and **2**.

Fluorescence activated cell sorting (FACS) analysis was performed[15] to investigate whether these synthetic compounds interact with gp120 inducing the conformational change necessary for the approach of an anti-envelope antibody or a co-receptor to the gp120. The profile of binding of an anti-envelope CD4-induced monoclonal antibody, 4C11, to the Env-expressing cell surface (an R5-HIV-1 strain, JR-FL,-infected PM1 cells) pretreated with the above CD4 mimic analogs was examined. Comparison of the binding of 4C11 to the cell surface was measured in terms of the mean fluorescence intensity (MFI), and is shown in Figure 2. Pretreatment of the Env-expressing cells with compound **2** (MFI = 38.42) produced a remarkable increase in binding affinity for 4C11, similar to that observed in pretreatment with sCD4 (MFI = 37.90). This is consistent with the results in the previous paper[10] where it was reported that compound **2** enhances the binding of gp120 to the 17b monoclonal antibody which recognizes the co-receptor binding site of gp120. Env-expressing cells, which were not pretreated with sCD4 or a CD4 mimic compound, did not show significant binding affinity for 4C11 (Fig. 2, blank). The increase in binding affinity for monoclonal antibodies may be due to conformational changes in gp120, which were caused by the interaction of sCD4 or a CD4 mimic with gp120. It is hypothesized that such conformational changes involve the exposure of the co-receptor binding site of gp120 (the V3 loop), which is hidden internally, since the binding of gp120 to 17b is enhanced. Compound **5**, which failed to show significant anti-HIV activity, and compounds **7**, **9** and **12**, which had significant anti-HIV activity, were assessed in the FACS analysis. The profile of the binding of 4C11 to the Env-expressing cell surface pretreated with compound **5** (MFI = 14.34) was similar to that of the blank (MFI = 11.24), suggesting that compound **5** offers no significant enhancement of binding affinity for 4C11. This result is compatible with the anti-HIV activity of compound **5**. The profile of the binding of 4C11 to the Env-expressing cell surface pretreated with compound **7** (MFI = 38.33) was entirely similar to that of compound **2** used as a pretreatment. Pretreatment of the cell surface with compounds **9** and **12** (MFI = 29.09 and 30.01, respectively) produced a slightly lower enhancement of binding affinity for 4C11, compared to those of compounds **2** and **7** as pretreatments. However, in the ITC experiments reported elsewhere,[10c] compound **9** (R = CF_3) has a high affinity for gp120, comparable to that of compound **2**, but compound **12** (R = NO_2) does not have significant affinity for gp120, indicating that these are not consistent with the current FACS studies, possibly due to the difference in the assay systems. Although the anti-HIV activity of **7** is weaker than that of compound **2**, the level of compound **7** inducing an enhancement of binding affinity of gp120 for 4C11 is comparable to that of compound **2**. The concentration of compounds used in the FACS analysis was 100 μM, much beyond the IC_{50} values of compounds **2** and **7**. A concentration of 100 μM would be also sufficient for the expression of anti-HIV activity caused by compounds **2** and **7**.

An effect on the use of compound **2** combined with another entry inhibitor was investigated. Analysis of the synergistic effects of anti-HIV agents was performed according to the median effect principle using the CalcuSyn version 2 computer program[18] to estimate IC_{50} values of compounds in different combinations. Combination indices (CI) were estimated from the data evaluated using the MTT assay

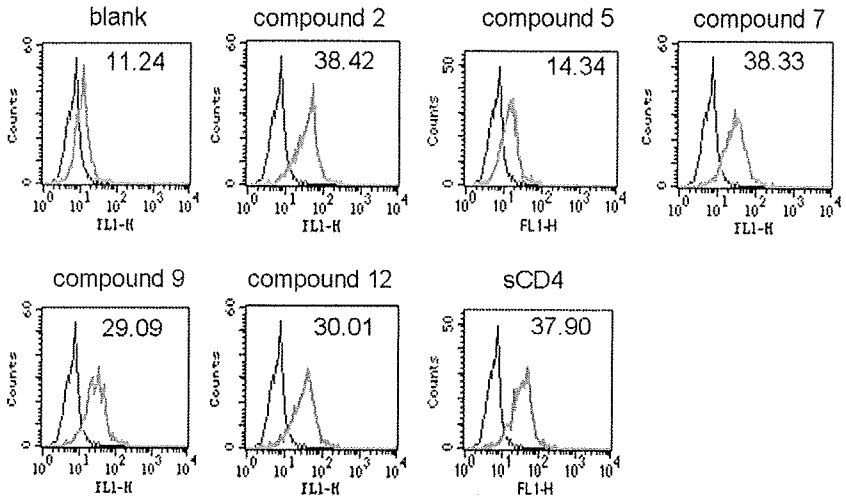

Figure 2. JR-FL (R5, Sub B) chronically infected PM1 cells were preincubated with 100 μM of a CD4 mimic or sCD4 (11 nM) for 15 min, and then incubated with an anti-HIV-1 mAb, 4C11, at 4 °C for 15 min. The cells were washed with PBS, and fluorescein isothiocyanate (FITC)-conjugated goat anti-human IgG antibody was used for antibody-staining. Flow cytometry data for the binding of 4C11 (green lines) to the Env-expressing cell surface in the presence of sCD4 or a CD4 mimic are shown among gated PM1 cells along with a control antibody (anti-human CD19: black lines). Data are representative of the results from a minimum of two independent experiments. The number at the top of each graph shows the mean fluorescence intensity (MFI) of the antibody 4C11.

Table 2
Combination indices (CI) for compound **2** or sCD4 and a CXCR4 antagonist, T140, against an HIV IIIB strain

Combination	HIV strain	CI values at different IC[a]		
		IC_{50}	IC_{75}	IC_{90}
2 + T140	IIIB	0.786	0.713	0.655
sCD4 + T140	IIIB	0.705	0.528	0.400

[a] The multiple-drug effect analysis reported by Chou et al. was used to analyze the effects of combinational uses of compounds.[18] CI <0.9: synergy, 0.9 < CI < 1.1: additivity, CI >1.1: antagonism.

(Table 2).[15] Compound **2** showed a highly remarkable synergistic anti-HIV activity with a co-receptor CXCR4 antagonist, T140,[8a] against an X4-HIV-1 strain, IIIB at various IC values (IC_{50}, IC_{75} and IC_{90}). However, sCD4 exhibited a higher synergistic effect (lower CI values) with T140 (Table 2). The interaction of sCD4 or a CD4 mimic with gp120 would expose the co-receptor-binding site of gp120, and the co-receptor CXCR4 could then easily approach gp120. Thus, an inhibitory effect of a CXCR4 antagonist would be meaningful, and a significant synergistic effect might also be brought about by a combination of sCD4 or a CD4 mimic and T140.

In summary, a series of CD4 mimic compounds were synthesized and evaluated for their anti-HIV activity. Several compounds showed significant anti-HIV activity with relatively low cytotoxicity. SAR studies showed that a certain level of size and electron-withdrawing ability of the substituents at the *p*-position of the phenyl ring are suitable for potent anti-HIV activity. In addition, the treatment of Env-expressing cells with several CD4 mimicking compounds causes a conformational change, exposing the co-receptor-binding site of gp120 externally. Thus, a CD4 mimic exhibited a remarkable synergistic effect with a co-receptor antagonist. These compounds are essential probes directed to the dynamic supramolecular mechanism of HIV entry, and important leads for the cocktail therapy of AIDS.

Acknowledgments

This work was supported by Mitsui Life Social Welfare Foundation, Grant-in-Aid for Scientific Research from the Ministry of Education, Culture, Sports, Science, and Technology of Japan, and Health and Labour Sciences Research Grants from Japanese Ministry of Health, Labor, and Welfare.

References and notes

1. Mitsuya, H.; Erickson, J. In *Textbook of AIDS Medicine*; Merigan, T. C., Bartlett, J. G., Bolognesi, D., Eds.; Williams & Wilkins: Baltimore, 1999; pp 751–780.
2. Chan, D. C.; Kim, P. S. *Cell* **1998**, *93*, 681.
3. (a) Alkhatib, G.; Combadiere, C.; Broder, C. C.; Feng, Y.; Kennedy, P. E.; Murphy, P. M.; Berger, E. A. *Science* **1996**, *272*, 1955; (b) Choe, H.; Farzan, M.; Sun, Y.; Sullivan, N.; Rollins, B.; Ponath, P. D.; Wu, L.; Mackay, C. R.; LaRosa, G.; Newman, W.; Gerard, N.; Gerard, C.; Sodroski, J. *Cell* **1996**, *85*, 1135; (c) Deng, H. K.; Liu, R.; Ellmeier, W.; Choe, S.; Unutmaz, D.; Burkhart, M.; Marzio, P. D.; Marmon, S.; Sutton, R. E.; Hill, C. M.; Davis, C. B.; Peiper, S. C.; Schall, T. J.; Littman, D. R.; Landau, N. R. *Nature* **1996**, *381*, 661; (d) Doranz, B. J.; Rucker, J.; Yi, Y. J.; Smyth, R. J.; Samson, M.; Peiper, S. C.; Parmentier, M.; Collman, R. G.; Doms, R. W. *Cell* **1996**, *85*, 1149; (e) Dragic, T.; Litwin, V.; Allaway, G. P.; Martin, S. R.; Huang, Y.; Nagashima, K. A.; Cayanan, C.; Maddon, P. J.; Koup, R. A.; Moore, J. P.; Paxton, W. A. *Nature* **1996**, *381*, 667.
4. Feng, Y.; Broder, C. C.; Kennedy, P. E.; Berger, E. A. *Science* **1996**, *272*, 872.
5. Wild, C. T.; Greenwell, T. K.; Matthews, T. J. *AIDS Res. Hum. Retroviruses* **1993**, *9*, 1051.
6. (a) Dorr, P.; Westby, M.; Dobbs, S.; Griffin, P.; Irvine, B.; Macartney, M.; Mori, J.; Rickett, G.; Smith-Burchnell, C.; Napier, C.; Webster, R.; Armour, D.; Price, D.; Stammen, B.; Wood, A.; Perros, M. *Antimicrob. Agents Chemother.* **2005**, *49*, 4721; (b) Price, D. A.; Armour, D.; De Groot, M.; Leishman, D.; Napier, C.; Perros, M.; Stammen, B. L.; Wood, A. *Bioorg. Med. Chem. Lett.* **2006**, *16*, 4633.
7. (a) Cahn, P.; Sued, O. *Lancet* **2007**, *369*, 1235; (b) Grinsztejn, B.; Nguyen, B.-Y.; Katlama, C.; Gatell, J. M.; Lazzarin, A.; Vittecoq, D.; Gonzalez, C. J.; Chen, J.; Harvey, C. M.; Isaacs, R. D. *Lancet* **2007**, *369*, 1261.
8. (a) Tamamura, H.; Xu, Y.; Hattori, T.; Zhang, X.; Arakaki, R.; Kanbara, K.; Omagari, A.; Otaka, A.; Ibuka, T.; Yamamoto, N.; Nakashima, H.; Fujii, N. *Biochem. Biophys. Res. Commun.* **1998**, *253*, 877; (b) Fujii, N.; Oishi, S.; Hiramatsu, K.; Araki, T.; Ueda, S.; Tamamura, H.; Otaka, A.; Kusano, S.; Terakubo, S.; Nakashima, H.; Broach, J. A.; Trent, J. O.; Wang, Z.; Peiper, S. C. *Angew. Chem., Int. Ed.* **2003**, *42*, 3251; (c) Tanaka, T.; Nomura, W.; Narumi, T.; Esaka, A.; Oishi, S.; Ohashi, N.; Itotani, K.; Evans, B. J.; Wang, Z.; Peiper, S. C.; Fujii, N.; Tamamura, H. *Org. Biomol. Chem.* **2009**, *7*, 3805.
9. Otaka, A.; Nakamura, M.; Nameki, D.; Kodama, E.; Uchiyama, S.; Nakamura, S.; Nakano, H.; Tamamura, H.; Kobayashi, Y.; Matsuoka, M.; Fujii, N. *Angew. Chem., Int. Ed.* **2002**, *41*, 2937.
10. (a) Zhao, Q.; Ma, L.; Jiang, S.; Lu, H.; Liu, S.; He, Y.; Strick, N.; Neamati, N.; Debnath, A. K. *Virology* **2005**, *339*, 213; (b) Schön, A.; Madani, N.; Klein, J. C.; Hubicki, A.; Ng, D.; Yang, X.; Smith, A. B., III; Sodroski, J.; Freire, E. *Biochemistry* **2006**, *45*, 10973; (c) Madani, N.; Schön, A.; Princiotto, A. M.; LaLonde, J. M.; Courter, J. R.; Soeta, T.; Ng, D.; Wang, L.; Brower, E. T.; Xiang, S.-H.; Do Kwon, Y.; Huang, C.-C.; Wyatt, R.; Kwong, P. D.; Freire, E.; Smith, A. B., III; Sodroski, J. *Structure* **2008**, *16*, 1689; (d) Haim, H.; Si, Z.; Madani, N.; Wang, L.; Courter, J. R.; Princiotto, A.; Kassa, A.; DeGrace, M.; McGee-Estrada, K.; Mefford, M.; Gabuzda, D.; Smith, A. B., III; Sodroski, J. *ProS Pathogens* **2009**, *5*, 1.
11. The structure of compound **2** was built in Sybyl and minimized with the MMFF94 force field and partial charges. (see: Halgren, T. A. *J. Comput. Chem.* **1996**, *17*, 490.) Docking was then performed using FlexSIS through its SYBYL

module, into the crystal structure of gp120 (PDB, entry 1RZJ). The binding site was defined as residues Val^{255}, Asp^{368}, Glu^{370}, Ser^{375}, Ile^{424}, Trp^{427}, Val^{430} and Val^{475}, and included residues located within a radius 4.4 Å. The ligand was considered to be flexible, and all other options were set to their default values. Figures were generated with ViewerLite version 5.0 (Accelrys Inc., San Diego, CA).

12. *For example, the synthesis of compound* **7**: To a solution of ethyl oxalyl chloride (0.400 mL, 3.48 mmol) in THF (20 mL) were added triethylamine (Et_3N) (0.480 mL, 3.48 mmol) and *p*-toluidine (373 mg, 3.48 mmol) with stirring at 0 °C. The reaction mixture was allowed to warm to room temperature, and then stirred for 6 h. After removal by filtration of the resulting salts, the filtrate was concentrated under reduced pressure. The residue was extracted with EtOAc (50 mL), and the extract was washed successively with brine (20 mL), 1 M HCl (20 mL × 2), brine (20 mL), saturated $NaHCO_3$ (20 mL × 2) and brine (20 mL × 3), then dried over $MgSO_4$. Concentration under reduced pressure gave the crude ethyl oxalamate, which was used without further purification. To a solution of the crude ethyl oxalamate (640 mg, 3.09 mmol) in THF (30 mL) were added aqueous 1 M NaOH (3.40 mL, 3.40 mmol), water (50 mL) and MeOH (20 mL) with stirring at 0 °C. The reaction mixture was allowed to warm to room temperature, and then stirred for 20 h. After the addition of aqueous 1 M HCl (5 mL), MeOH and THF were evaporated under reduced pressure. The residue was acidified to pH 2 with 1 M HCl, and extracted with EtOAc (50 mL × 2). The combined organic layer was washed with brine (20 mL × 3), and dried over $MgSO_4$. Concentration under reduced pressure gave the crude acid, which was used for the next reaction without further purification. To a solution of the above crude acid (514 mg, 2.87 mmol) in THF (10 mL) were added 1-hydoxybenzotriazole (484 mg, 3.16 mmol), 4-amino-2,2,6,6-tetramethylpiperidine (446 μL, 2.58 mmol), 1-ethyl-3-(3-dimethylaminopropyl)carbodiimide hydrochloride (606 mg, 3.16 mmol) and Et_3N (0.439 mL, 3.16 mmol) with stirring at 0 °C. The reaction mixture was allowed to warm to room temperature, and then stirred for 20 h. After evaporation of THF, the residue was dissolved in $CHCl_3$ (50 mL). The mixture was washed with saturated $NaHCO_3$ (20 mL × 2) and brine (20 mL × 3), and dried over $MgSO_4$. Concentration under reduced pressure gave the crude crystalline mass. The usual work-up followed by recrystallization from EtOAc–*n*-hexane gave the title compound **7** (363 mg, 1.14 mmol, 39.8%) as colorless crystals, mp = 176 °C; δ_H (400 MHz; $CDCl_3$) 1.07 (1H, m, NH), 1.16 (6H, s, CH_3), 1.29 (6H, s, CH_3), 1.44 (2H, m, CH_2), 1.91 (1H, d, *J* 3.7, C*H*H), 1.94 (1H, d, *J* 3.7, CH*H*), 2.34 (3H, s, CH_3), 4.25 (1H, m, CH), 7.17 (2H, d, *J* 8.3, ArH), 7.33 (1H, m, NH), 7.50 (2H, d, *J* 8.4, ArH), 9.18 (1H, s, NH); HRMS (FAB), *m/z* calcd for $C_{18}H_{28}N_3O_2$ $(MH)^+$ 318.2182, found 318.2173.
13. McFarland, C.; Vicic, D. A.; Debnath, A. K. *Synthesis* **2006**, 807.
14. *The synthesis of compound* **12**: To a solution of Et_3N (417 μL, 3.00 mmol) and 4-nitroaniline (138 mg, 1.00 mmol) in THF (1.3 mL) was added oxalyl dichloride (85.8 μL, 1.00 mmol) with stirring at 0 °C. After being stirred for 30 min at 0 °C, Et_3N (167 μL, 1.20 mmol) and 4-amino-2,2,6,6-tetramethylpiperidine (156 μL, 0.90 mmol) were added. The reaction mixture was stirred for 6 h at 0 °C. After removal by filtration of the resulting salts, the filtrate was concentrated under reduced pressure. The residue was dissolved in $CHCl_3$ (20 mL), and the mixture was washed successively with brine (10 mL), saturated $NaHCO_3$ (10 mL × 2) and brine (10 mL × 3), and dried over $MgSO_4$. Concentration under reduced pressure followed by flash chromatography over silica gel with $CHCl_3$–MeOH (9:1) gave 42.4 mg (0.122 mmol, 13.5%) of the title compound **12** as colorless crystals, mp = 190 °C; δ_H (400 MHz; $CDCl_3$) 1.09 (1H, m, NH), 1.17 (6H, s, CH_3), 1.29 (6H, s, CH_3), 1.43 (2H, m, CH_2), 1.92 (1H, d, *J* 3.8, C*H*H), 1.95 (1H, d, *J* 3.8, CH*H*), 4.28 (1H, m, CH), 7.29 (1H, m, NH), 7.82 (2H, d, *J* 9.1, ArH), 8.28 (2H, d, *J* 9.1, ArH), 9.55 (1H, s, NH); HRMS (FAB), *m/z* calcd for $C_{17}H_{25}N_4O_4$ $(MH)^+$ 349.1876, found 349.1871.
15. Yoshimura, K.; Shibata, J.; Kimura, T.; Honda, A.; Maeda, Y.; Koito, A.; Murakami, T.; Mitsuya, H.; Matsushita, S. *AIDS* **2006**, *20*, 2065.
16. (a) Chapman, N. B.; Shorter, J. *Advances in Linear Free Energy Relationship*; Plenum Press: London, 1972; (b) Chapman, N. B.; Shorter, J. *Correlation Analysis in Chemistry*; Plenum Press: London, 1978; (c) Hansch, C.; Leo, A. J.; Hoekman, D. *Exploring QSAR, Hydrophobic, Electronic, and Steric Constants*; American Chemical Society: Washington, DC, 1995.
17. Taft, R. W. In *Steric Effects in Organic Chemistry*; Newman, M. S., Ed.; John Wiley: New York, 1956; p 556.
18. (a) Chou, T. C.; Talalay, P. *J. Biol. Chem.* **1977**, *252*, 6438; (b) Chou, T. C.; Hayball, M. P. *CalcuSyn*, 2nd ed.; Biosoft: Cambridge, UK, 1996.

JGV Papers in Press. Published December 23, 2009 as doi:10.1099/vir.0.017426-0

HIV-1 evasion of a neutralizing anti-V3 antibody involves acquisition of a potential glycosylation site in V2.

Makiko Hatada, Kazuhisa Yoshimura, Shigeyoshi Harada, Yoko Kawanami, Junji Shibata and Shuzo Matsushita*

Division of Clinical Retrovirology and Infectious Diseases, Center for AIDS Research, Kumamoto University, Kumamoto 860-0811, Japan

Running title: Neutralizing antibody evasion of HIV-1

*Corresponding author:

Shuzo Matsushita

Division of Clinical Retrovirology and Infectious Diseases, Center for AIDS Research, Kumamoto University, Kumamoto 860-0811, Japan

Phone: +81-96-373-6536

Facsimile: +81-96-373-6537

E-mail: shuzo@kumamoto-u.ac.jp

Summary: 240 words, Main text: 5459 words, 6 figures, 2 tables and 1 supplementary data.